Graduate School ETD Form 9
(Revised 12/07)

PURDUE UNIVERSITY
GRADUATE SCHOOL
Thesis/Dissertation Acceptance

This is to certify that the thesis/dissertation prepared

By NIDA TANATAWEETHUM

Entitled

Mechanical Property and Biocompatibility of PLLA Coated DCPD Composite Scaffolds

For the degree of Master of Science in Biomedical Engineering

Is approved by the final examining committee:

Tien-Min Chu
Chair

Chien-Chi Lin

Marco C. Bottino

To the best of my knowledge and as understood by the student in the *Research Integrity and Copyright Disclaimer (Graduate School Form 20)*, this thesis/dissertation adheres to the provisions of Purdue University's "Policy on Integrity in Research" and the use of copyrighted material.

Approved by Major Professor(s): Tien-Min Chu

Approved by: Edward Berbari 11/20/2013
Head of the Graduate Program Date

MECHANICAL PROPERTY AND BIOCOMPATIBILITY OF PLLA COATED DCPD COMPOSITE SCAFFOLDS

A Thesis
Submitted to the Faculty
of
Purdue University
by
Nida Tanataweethum

In Partial Fulfillment of the
Requirements for the Degree
of
Master of Science in Biomedical Engineering

December 2013
Purdue University
Indianapolis, Indiana

ACKNOWLEDGEMENTS

Firstly, I would like to extend my greatest gratitude to my advisor, Dr. T. M. Gabriel Chu, for all the guidance, advice, and financial assistance throughout my thesis research. His abundance of knowledge and experience has helped me a lot even in my harshest time.

I would also like to extend recognition to my committee members, Dr. Marco Bottino and Dr. Chien-Chi Lin for their time, great advice, and participating in my thesis defense. Their advice and comments further enhanced the quality of my thesis contents.

I would also like to extend my appreciation to Dr. Wai-Ching Liu, Ms. Meoghan MacPherson, and my lab collaborator for their advice and assistance. I give special thanks to Ms. Valerie Lim Diemer for her aid and guidance for preparing my thesis.

Finally, I want to dearly thank my family for their love, priceless advice, and their support throughout my education. Thank my friends for their love and warm support. The encouragement I received will be forever remembered and appreciated. Thank you all.

TABLE OF CONTENTS

Page

Page

LIST OF TABLES

LIST OF FIGURES

Figure Page

Figure Page

ABSTRACT

Tanataweethum, Nida. M.S.B.M.E., Purdue University, December 2013. Mechanical Property and Biocompatibility of PLLA Coated DCPD Composite Scaffolds. Major Professor: T.M. Gabriel Chu.

Dicalcium phosphate dihydrate (DCPD) cements have been used for bone repair due to its excellent biocompatibility and resorbability. However, DCPD cements are typically weak and brittle. To overcome these limitations, the sodium citrate used as a setting regulator and the coating of poly-L-lactide acid (PLLA) technique have been proposed in this study. The first purpose of this thesis is to develop composite PLLA/ DCPD scaffolds with enhanced toughness by PLLA coating. The second purpose is to examine the biocompatibility of the scaffolds. The final purpose is to investigate the degradation behaviors of DCPD and PLLA/DCPD scaffolds. In this experiment, DCPD cements were synthesized from monocalcium phosphate monohydrate (MCPM) and β-tricalcium phosphate (β –TCP) by using deionized water and sodium citrate as liquid components. The samples were prepared with powder to liquid ratio (P/L) at 1.00, 1.25 and 1.50. To fabricate the PLLA/DCPD composite samples, DCPD samples were coated with 5 % PLLA. The samples were characterized mechanical properties, such as porosity, diametral tensile strength, and fracture energy. The mechanical properties of DCPD scaffolds with and without PLLA coating after the in vitro static degradation (day 1, week 1, 4, and 6) and in vitro dynamic degradation (day 1, week 1, 2, 4, 6, and 8) were investigated by measuring their weight loss, fracture energy, and pH of phosphate buffer solution. In addition, the dog bone marrow stromal stem cells (dBMSCs) adhesion on DCPD and PLLA/DCPD composite samples were examined by scanning electron microscopy. The cell proliferation and differentiation in the medium conditioned with DCPD and PLLA/DCPD composite samples were studied by XTT (2,3-Bis(2-methoxy-4-nitro-5-sulfophenyl)-2H-tetrazolium-5-carboxanilide inner salt), and alkaline phosphatase

(ALP) assay, respectively. The addition of sodium citrate and PLLA coating played a crucial role in improving the mechanical properties of the samples by increasing the diametral tensile strength from 0.50 ± 0.15 MPa to 2.70 ± 0.54 MPa and increasing the fracture energy from 0.76 ± 0.18 N-mm to 12.67 ± 4.97 N-mm. The DCPD and PLLA/DCPD composite samples were compatible with dBMSCs and the cells were able to proliferate and differentiate in the conditioned medium. The degradation rate of DCPD and PLLA/DCPD samples were not significant different ($p > 0.05$). However, the DCPD and PLLA/DCPD composite samples those used sodium citrate as a liquid component was found to degrade faster than the groups that use deionized water as liquid component

1. INTRODUCTION

1.1 Calcium Phosphate Cements in Bone Tissue Engineering

Musculoskeletal diseases, such as arthritis, osteoporosis, bone fractures and traumas annually cost United States over $250 billion and affect people more than hundred millions across the world. About 10 million Americans already have osteoporosis, and 34 million are at risk of this disease. In 2005, two million fractures due to osteoporosis, which cost over $19 billion, were estimated. Moreover, three million fractures and over $25 billion in costs each year will be expected by 2025 [1]. Considering the terrible impact of musculoskeletal diseases on the economy and the population illustrates the importance of progressing the understanding of musculoskeletal disorders through the education and research to improve the quality of life with better musculoskeletal conditions. Therefore, the field of tissue engineering has been marvelously advanced recently since being described by Vacanti et al. [2] in 1993 as the application of "the principles of engineering and the life sciences toward the development of biological substitutes that restore, maintain, or improve tissue function". Although a range of hard tissues including bones and cartilages has been researched, the clinical application of engineered hard tissues has been limited. The several current therapies of reconstruction of bone defects have been applied, such as autografting and allografting, However, these standard treatments still have some limitations. Although bone grafts are avascular and depend on the diffusion, the size of defects and the shortage of donors still limit these applications. Furthermore, the unpredictable bone resorption will be difficult for bone volume maintenance. In large defects, the grafts resorption will be completed before osteogenesis is achieved [3]. In addition, the autografting is also limited by the additional morbidities due to bone harvesting [4]. A high failure rate of allografts was shown due to the risk of disease transmission [3]. These significant

drawbacks drive researchers in bone tissue engineering to challenge developing new materials for bone grafts and scaffolds that allow for minimally invasive surgical methods and provide some of the similar responses to bone. Calcium phosphate cements (CPCs) are one of the most interesting materials for scaffolds due to their similarity of bone mineral phase and the nature of setting in situ [5]. Therefore, calcium phosphate cements (CPCs) have been considered as a bone-defect repair material.

Calcium phosphate cements (CPCs) were discovered in the early eighties by Brown and Chow [6] and LeGeros et al. [7]. They have been categorized into two types: apatite CPCs and brushite CPCs. Although both of them are biocompatible, brushite CPCs have better resorbability in vivo than apatite CPCs [8].

CPCs are very versatile materials, which draw attention among researchers due to their advantages over calcium phosphates ceramic in comparison [9]. First is their capacity of self-setting in vivo. Second, their injectability creates excellent prospects for minimally invasive surgical techniques. Third, CPCs can be shaped to fit the implant site ensuring the good bone-material contact to allow the optimum tissue-biomeaterial contact for activating the bone in growth. Fourth, the dissolution- precipitation process, which takes place under in vivo condition, brings about interconnected micro porosity, chemistry, and structure, which are similar to biological apatites. Finally, the low-temperature setting reaction allows CPCs to be incorporated with various drugs, such as antibiotics and anti-inflammatory drugs. However, CPCs also have some limitations related to their poor mechanical properties, which diminish their applicability from load bearing applications [10].

1.2 Statement of Research Question

First of all, brushite cements have some critical drawbacks; their brittleness and low mechanical strength limiting them from load bearing applications. In this research, poly-l-lactide acide (PLLA) coated on dicalcium phosphate dihydrate (DCPD) technique

was proposed to improve the toughness of DCPD scaffolds. Moreover, different ratios of powder to liquid were determined to improve the mechanical property of DCPD scaffolds. In addition, sodium citrate was used as liquid regulator for DCPD preparation to improve the mechanical tensile strength of DCPD scaffolds.

Secondly, a critical concern for the development of DCPD scaffolds is the degradation of brushite cements. Several studies have shown that DCPD were rapidly resorbed under physiological condition [8]. In this study, PLLA coating technique was applied to construct the DCPD scaffolds to slow down the degradation of these scaffolds during in vitro degradation under both static and dynamic conditions.

Finally, The biocompatibility of brushite cements was well documented under in vivo conditions [11, 12]. However, there are only few research focus on the in vitro biocompatiblity of DCPD cements [13]. In this study, DCPD and composite PLLA/DCPD composite disk samples were fabricated to investigate the biocompatibility of the scaffolds.

1.3 Thesis Overview

Chapter 2 provides the overview of the expanding researches for brushite calcium phosphate cements. This chapter begins with the classification of calcium phosphate cements based on chemical makeup and reaction mechanism. In order to evaluate the mechanical property of brushite cements, the current standard methods were explained in mechanical property analysis section: diametral tensile strength. Next is to summarize the current techniques applying for improving the mechanical properties of brushite cements. Finally, the DCPD degradation properties were stated in this chapter.

Chapter 3 provides experimental details to study the effect of material parameters, such as the ratios of β tricalcium phosphate (β-TCP) and monocalcium phosphate monohydrate (MCPM), size of samples and percentage of PLLA coating. In this chapter,

porosity, diametral tensile strength, and fracture energy of the DCPD and PLLA/DCPD samples were used to criteria to determine the optimum condition for further experiments.

Chapter 4 provides further experimental details to investigate the effects of setting regulator. Sodium citrate was used as a setting regulator to improve the mechanical property of DCPD disk samples. Three material parameters were determined in this study: porosity, diametral tensile strength and energy to fracture. In addition, these parameters were used to evaluate the best condition for 3D scaffolds.

Chapter 5 provides experiment details about the effect of PLLA infiltration on DCPD disk samples under in vitro static and dynamic degradations. In this experiment, pH value, percentage of weight loss and energy to fracture of the disk samples were investigated during different degradation periods.

Chapter 6 states further experimental information about the cytocompatibility of DCPD and PLLA/DCPD composite disk samples. Dog bone marrow stromal stem cells were used in this study to investigate the cell morphology, proliferation, and differentiation.

2. FOUNDATIONS IN CURRENT CALCIUM PHOSPHATE RESEARCH

2.1 Introduction

The increase in the rate of bone fractures have been observed with the aging population [14]. Implantation of a temporary or permanent prosthesis, which is a challenge for the orthopedic surgeon especially in a large bone defect case, is highly demanded for operative treatments. An increasing of bone fractures from high aging population and the limitation of bone grafts result in the high clinical demand for bone substitutes. Bone substitute materials should be biocompatible, biodegradable at the expense of bone growth, and moldable for restoring bone defects [15]. One interesting material meeting these requirements is calcium phosphate cement.

2.2 Classification of Calcium Phosphate Cements

Calcium phosphate cements (CPCs) were discovered by Brown and Chow [16] and LeGeros et al. [7] in early eighties. This material has attracted much attention from several researchers in bone tissue engineering due to their salient advantages: the ability to form direct bond with bone and the low temperature of self-setting reaction under physiological conditions [9]. There are two major types of CPCs: apatite cements and brushite cements. Apatite cements were studied by several research groups due to their resemblance to bone mineral. Moreover, they have more favorable mechanical properties and stability at higher pH (pH > 4.2) than brushite (pH < 4.2) [17]. However, brushite (dicalcium phosphate dihydrate, DCPD) has been shown for the better ability to resorb in vivo over apatite and also promised a material for bone defect filling [8]. DCPD will be focused in this study.

The main composition of dicalcium phosphate cements is alkaline calcium source, acidic phosphate source, and water. The additive components are also mixed to improve the mechanical properties and setting time.

2.2.1 Alkaline Calcium Sources

Alkaline calcium source in dicalcium phosphate, such as calcium oxide and calcium hydroxide are basic [8]. Since the calcium to phosphate ratio in brushite is equal to 1, the calcium phosphate compounds containing higher ratios of calcium to phosphate can be used as alkaline calcium source for these cements. The most general alkaline calcium source for brushite is tricalcium phosphate (TCP) (ratio of calcium to phosphate = 1.5), which have two crystallographic forms: β-TCP and α-TCP [8]. For this reason, β-TCP is more frequently used in brushite cements because it requires lower energy for its production [8]. In addition, β-TCP was used to prepare DCPD in this study. Table 2.1 summarizes the common alkaline calcium components for dicalcium phosphate.

2.2.2 Acidic Phosphate Sources

The acidic calcium phosphates used for dicalcium phosphate preparation should have a calcium to phosphate ratio lower than one [8]. Since monoclcium phosphate monohydrate (MCPM) and monocalcium phosphate anhydrous (MCPA) are the two only calcium phosphates that can meet the requirements, they are frequently used for dicalcium phosphate preparation [8]. In addition, phosphoric acid is another acidic phosphate source commonly used for dicalcium phosphate preparation due to its low cost [8]. However, MCPM was used to prepare DCPD in this study due to the novel formulation from previous study [18]. Table 2.2 summarizes the general acidic phosphate components for dicalcuim phosphate [8].

Table 2.1 The summary of the alkaline calcium sources for dicalcium phosphate cements.

Alkaline calcium component	
Name	Chemical Formula
Alpha tricalcium phosphate (α-TCP)	$\propto$-$Ca_3(PO_4)_2$
Beta tricalcium phosphate (β-TCP)	β-$Ca_3(PO_4)_2$
Calcium oxide	CaO
Calcium hydroxide	$Ca(OH)_2$

Table 2.2 The summary of the acidic phosphate sources for dicalcium phosphate cements.

Acidic phosphate component	
Name	Chemical Formula
Monocalcium phosphate monohydrate (MCPM)	$Ca(H_2PO_4)_2 \cdot H_2O$
Phosphoric acid (PA)	H_3PO_4
Monocalcium phosphate anhydrous (MCPA)	$Ca(H_2PO_4)_2$
Pyrophosphoric acid (PyA)	$H_4P_2O_7$

2.2.3 Additives

Besides the reagents required for brushite cements formation, several additives are needed to improve the properties of the cements. These additives are usually added to the powder or liquid component during cement mixing to improve the setting time and mechanical properties. In addition, they are also used to activate the precipitation of cements. Table 2.3 summarizes the general additives and their functions. In addition, more effects of the additives on cements will be described in later sections [8].

Table 2.3 The summary of the additives for dicalcium phosphate cements.

Additive	Function
Sulfuric Acid	Setting time, Mehcanical properties
Sodium pyrophosphate	Setting time, Mehcanical properties
Citric acid	Setting time, Mehcanical properties
Sodium citrate	Setting time, Mehcanical properties
Magnesium sulfate	Setting time, Mehcanical properties
Tartaric acid	Setting time, Mehcanical properties
Pyrophosphoric acid	Setting time, Mehcanical properties
Glycolic acid	Setting time, Mehcanical properties
Disodium hydrogen phosphate	Setting time, Mehcanical properties
Sodium dihydrogen phosphate	Setting time, Mehcanical properties

2.3 Chemical Reactions

Brushite (Dicalcium phosphate dihydrate, DCPD) cement chemical setting reaction consists of four steps: the first one is the dissolution of the cement powder into a solvent, the second step is the formation of a super-saturated gel, the third step is the nucleation within the gel, and the final step is the growth crystals to a solid of interlocked crystals [19].

The first step starts when MCPM is exposed to the water and hydrolyzed to diphosphate and calcium ions following an endothermic reaction (23.0 kJ mole^{-1}) (2.1) [19]. Simultaneously, the dissolution of β-TCP occurrs under exothermic reaction (-66.0 kJ mole^{-1}) due to the acid exposure from the dissolution of MCPM (2.2) [19]. After the initial dissolution of the reagents, the brushite cements are precipitated to form crystals under exothermic reaction (-10.0 kJ mole^{-1}) (2.3) [19]. Finally, Equation 2.4 is derived from Equation (2.1) + (2.2) + (4* (2.3)), which is exothermic reaction (-83.3 kJ mole^{-1}) [19].

$$Ca(H_2PO_4)_2 \cdot H_2O \rightarrow Ca^{2+} + 2H_2PO_4^- + H_2O \quad (2.1)$$

$$\beta - Ca_3(PO_4)_2 + 4H^+ \rightarrow 3Ca^{2+} + 2H_2PO_4^- \quad (2.2)$$

$$Ca^{2+} + H_2PO_4^- + 2H_2O \rightarrow CaHPO_4 \cdot 2H_2O + H^+ \quad (2.3)$$

$$\beta - Ca_3(PO_4)_2 + Ca(H_2PO_4)_2 \cdot H_2O + 7H_2O \rightarrow 4(CaHPO_4 \cdot 2H_2O) \quad (2.4)$$

The final setting of DCPD cements from β-TCP and MCPM was reported that this setting system took few minutes after mixing [20]. In addition, the nuclear magnetic resonance spectroscopy (NMR) study indicated that MCPM completely reacted under the chemical setting reaction within the first 20 minutes while some β-TCP was left under unreacted condition [21].

2.4 Setting Time Modification

Brushite cements have remarkable resorbability and biocompatibility. Since they were metastable under physiological conditions, they degraded faster than apatite after implantation [22]. However, their short setting times and low mechanical properties limit them from broader clinical applications.

The setting times of brushite cements depend on the solubility of a basic phase or the alkaline calcium components. The higher solubility of the basic phase yields faster setting time. The setting time of brushite cements depends the solubility of alkaline calcium components. For instance, the solubility of α-TCP is higher than β-TCP. MCPM + β-TCP needed 30-60 seconds for the setting reaction. In contrast, MCPM + α-TCP needed only few seconds for the setting reaction [15].

The additives with regarded to Table 2.3 can be applied to modify the setting reaction of brushite cements. They inhibit the dissolution of the reagents and the precipitation of the crystals [8]. The citrate ions inhibit the dissolution of β-TCP and MCPM during formation of cements [19]. These effects were demonstrated by the reduction of the exothermic heat from the cement precipitation leading to the prolonged setting time [19].

Brushite crystal is a non-centrosymmetrical monoclinic plate, which has the morphology dominated by (0 1 0) faces, consist of two rows of Ca^{2+} and PO_4^{2-}. In addition, there are the bonds of layers of water molecules between the calcium phosphate sheets. The additives interfere with phosphate incorporation during precipitation limiting the crystal growth and the kinetics of growth [8]. Several pyrophosphate compounds and sulfate ions are applied to prolong the setting time, such as sodium pyrophosphate, pyrophosphoric acid, sulfuric acid, and magnesium sulfate. The addition of low concentration of sulfate ions to form the cements can delay the setting time. However, the addition of high concentration of sulfate ions resulting in formation of calcium sulfate dehydrate crystals acting as the nuclei to accelerate the crystallization of brushite cements [8]. The α-hydroxyl carboxylic acids, such as citric acid, tartaric, and glycolic acid can bind to calcium ions to regulate the growth of brushite crystals resulting in the prolonged setting time [8].

2.5 Mechanical Property Modification

According to the standards of American Society for Testing and Materials (ASTM 5833, 2002), the brushite cements are required to at least set for twenty-four hours before testing the mechanical properties for bone cements [8]. In addition, the cement should be set and dried under dry condition (room temperature and humidity). Two types of mechanical measurement are used to test the mechanical properties of the cements: compressive strength and tensile strength. The brittle materials are difficult to test for the direct tensile strength. Therefore, several studies measured the diametral tensile strength instead of the direct tensile strength. The mechanical performance of dicalcium phosphate cement under compression forces was better than under tensile strains [8].

Small particle sizes of the reagents are applied to improve the mechanical properties of the cements. The compressive strength of DCPD cements was increased to 52 MPa (more than 100%) by adjusting the particle sizes of MCPM and β-TCP [23].

The compressive strength and diametral tensile strength of the cements have inverse relationships with their porosity. In addition, reducing porosity results in more compaction of the cements and higher strength [8]. The powders to liquid (P/L) ratios were applied to regulate the porosity of the cements. A low P/L ratio results in an excess of water in the setting reaction yielding too high porosity and low mechanical strength. On the contrary, a high P/L ratio results in the improperly mixed cements. Therefore, the additives used as the setting regulator are required to improve the mixing condition of cements [8].

The degree of cement setting has a significant effect on its mechanical properties. Longer cements setting time yield the higher strength. The additives that used as the retardants in the setting systems in regarded to Table 2.3 are applied to improve cements' mechanical properties [8].

The pyrophosphate salts, α-hydroxyl carboxylic acids, and their salts, such as sodium citrate, citric, glycolic and tartaric acids were applied to improve the cements mixing with the higher P/L ratios to increase the strength of the cements. However, the concentration of these additives needs to be determined to obtain the optimality.

A critical limitation of the cements is their low mechanical properties. Since they are brittle, they have low impact resistance and low tensile strength (6 to 10 MPa) [24]. On the other hand, their compressive strengths were higher than normal bones after implanted for twelve weeks (60-70 MPa) [24]. Moreover, the addition of water soluble polymers to the cement liquid phase during cement mixing were applied to improve the mechanical properties. For example, polyacrylic acid and polyvinyl alcohol were used to improve the mechanical properties of a TTCP + DCPD cement. The results showed that the mechanical properties of the cements were remarkably increased (up to three folds) while the setting time significant decreased [25]. In addition, hydrophobic polymer can be added to the cement mixture to increase the tensile strength. Gorst et al. reported that the addition of polyglactin (PGA) in the form of reinforcing fibers with the optimal

arrangement of these fibers on the tensile surface of the cement matrix resulting in the increase of the flexural strength up to 7-fold [26]. However, in the case of the fabrication of calcium phosphate cement scaffold via casting method, the incorporation of polymer during cement mixing might inhibit the casting ability of the cements by blocking the channels of the scaffold molds [27].

Another method to improve the mechanical properties of the calcium phosphate cement (CPC) scaffolds is to coat a thin layer of the polymer on the CPC scaffolds. However, few studies have applied this technique to the CPC scaffolds. The 3D DCPD scaffolds coated with poly(ethylene glycol) diacrylate (PEGDA) showed the improvement of flexural strength from 0.44 ± 0.12 MPa to 7.04 ± 0.51 MPa [27]. Moreover, DCPD scaffolds coated with poly(propylene fumarate) (PPF) reported the increase of the flexural strength from 1.80 ± 0.19 MPa to 16.14 ± 1.70 MPa [28].

In this project, poly-L-lactic acid (PLLA) was chosen to coat on the DCPD samples to improve the diametral tensile strength and fracture energy due to its following excellent properties. PLLA has been showed to have excellent biocompatibility and degradability. Xuan et al. revealed that PLLA had very low degradation rate when examining a PLLA with molar mass = 100-300 kDa and percent crytallinity of 50%, which was slower than other synthetic polyesters, such as poly(glycolic acid-co-lactic acid) and polyglycolic acid (PGA) [29]. In addition, PLLA were non-cytotoxic and not totally biological inert. Macrophages and multinucleated giant cells were found to appear on the surface of PLLA screws implanted in the sheep bone [30].

2.6 Current Mechanical Characterization

The demand of the scaffolds for repairing load-bearing bone defects, especially large defects, is apparent. In order for the scaffolds to handle the load in cortical and trabecular bones, the scaffolds should have the mechanical properties that match to those of the natural bone and must be able to maintain the high level of mechanical stability during

the implantation. The target properties, such as the diametral tensile strength, fracture energy, and the degradation of the scaffolds must be optimized to design the scaffolds that account for both the change of properties with the degradation and the change with the expected bone ingrowth.

2.6.1 In Vitro Degradation

Several studies have shown that brushite cements resorbed much faster under physiological compared to hydroxyapatite cements [8]. This is one of the most interesting advantages of brushite cements. Therefore, it is crucial to understand the mechanism of brushite resorption. The degradation of the DCPD consists of 3 mechanisms: dissolution, disintegration, and conversion [31-33]. The dissolution starts when the DCPD is placed into the solution containing under saturated calcium and phosphate ions. The dissolution mechanism leads to the mass loss in DCPD and the decrease of pH values based on the following equation:

$$CaHPO_4 \cdot 2H_2O \rightarrow Ca^{2+} + HPO_4^{2-} + 2H_2O \quad (2.5)$$

The high level of DCPD dissolution results in the disintegration of the cements according to the changing of its microstructure [33, 34]. In addition, the rate of dissolution of the ions from DCPD crystals also depends on the chemical equilibrium between the dissolution and recrystallization [32]. Once the solution reaches to the equilibrium, the dissolution of DCPD will stop and the mass and pH will stabilize [31, 33]. In the case of dynamic degradation, the calcium and phosphate ions will be removed from the solution resulting in the further dissolution of DCPD and the reprecipitation of DCPD as HA [33]. In the case of static degradation, the solution will become supersaturated with calcium and phosphate ions resulting the conversion of DCPD to HA based on Equation 2.6 [31, 33].

$$10CaHPO_4 \cdot 2H_2O \rightarrow Ca_{10}(PO_4)_6(OH)_2 + 4H_3PO_4 + 18H_2O \quad (2.6)$$

The conversion of DCPD to HA results in the formation of phosphoric acid, which results in the decreasing of pH values and an increase of solubility of DCPD due to their metastable structure at pH > 4.2 [10].

In the excess of β-TCP, the final composition is the mixture of DCPD and unreacted β-TCP. The resorption of the unreacted β-TCP is slower than DCPD. In addition, it remains low and stable for long period of time [35]. However, glycolic acid (1 carboxylic group), tartaric acid (2 carboxylic groups) and citric acid (3 carboxylic groups) were used to help the disintegration of β-TCP. In addition, the more soluble calcium carboxylate was found in the solution, the more β-TCP was released [32].

2.6.2 Diametral Tensile Strength

Brushite cements are known as bone-resembling materials with the excellent resorption under physiological conditions and biocompatibility but limited mechanical strength [8]. Since one of the important functions of the bone is to support the load in the body, the mechanical strength of the brushite cements should be improved and analyzed.

Bone graft and scaffolds are subjected to complex loading in the body, including combinations of compression and tension. While cement is strong in compression, its tensile strength is usually low and therefore plays a limiting factor in its mechanical behavior in vivo. Direct tensile strength of brittle materials is difficult to be measured. Therefore, diametral tensile strength is another alternative for tensile measurement.

Demetral tensile strength is known as the indirect tension test for brittle materials, such as ceramics and concrete. This test was developed by Carneiro and Barcellos in 1952 [36]. The test was proceeded by applying the compression load along two opposite generators (diametral plane) on the cylinder as shown in Fig. 3.1. The diametral tensile strength can be derived from the Equation 3.2.

Chow et al. reported that the effect of applying the pressure to the Calcium phosphate cements during molding. The cement pastes at P/L = 4.0 were placed into the molds and the range of pressure 0-2.8 MPa were applied with the different length of time (0.5-4 h). The diametral tensile strength was found to be significantly affected by the pressure while no significant effect was found by the time [16].

Van Landuyt et al. indicated that diametral tensile strength was related to the conversion of the initial β-TCP to the DCPD cements. In addition, the higher initial MCPM contents promoted the higher coversion of β-TCP to the DCPD cements resulting in lower porosities. Moreover, the optimal diametral tensile strength of DCPD cements was achieved at 2.5 MPa [37].

Faleh et al demonstrated that glycolic acid and citric acid delayed the time of the setting reaction and limited the cement crystals growth resulting in the more compaction of the cements and the increase in the diametral tensile strength. Moreover, the additional $\propto$ hydroxyl group in carboxylic acid and the solubility of the calcium salt are the main factors to limit the brushite setting reaction [20].

3. MECHANICAL CHARACTERIZATION OF DICALCIUM PHOSPHATE DIHYDRATE CEMENTS

3.1 Introduction

Dicalcium phosphate dihydrate cements (DCPD) have been widely used as bone filling materials owing to their remarkable biocompatibility and bioresorbability. However, the low mechanical strength (1 MPa diametral strength) restricted them from broader clinical applications [8]. A thin layer of polymer coating is a method applied to improve toughness of scaffolds [38, 39]. In this research, poly (L-lactic acid) coating technique was applied to DCPD samples fabrication due to their mechanical property, biocompatibility and biodegradability [40].

Two types of mechanical assessments have been tested to analyze their mechanical properties: diametral tensile strength and fracture energy. Diametral tensile strength was measured in this study instead of direct tensile strength due to the difficulty in measurement of brittle material even though the measurement of diametral tensile strength yield the result of 85% of the true strength of cements [8]. Fracture energy was investigated in this study to identify the toughness of the materials. Since porosity was inversely correlated to diametral tensile strength of brushite cements, powder to liquid ratios were varied in this experiment to adjust the porosity for DCPD samples fabrication.

In this experiment, the ratios of monocalcium phosphate monohydrate (MCPM)/β-Tricalcium phosphate (β-TCP) were varied to fabricate DCPD samples in order to obtain DCPD samples with high diametral tensile strength. In addition, two designs of samples were created and investigated to determine the better designs for further experiment. Finally, different percentages of PLLA were coated on the samples to investigate the fracture energy of DCPD samples.

3.2 Sample Preparation

Firstly, six groups of DCPD cylindrical samples with different MCPM/β-TCP ratios and different powder to liquid (P/L) ratios were fabricated as shown in Table 3.1 to investigate the correlation between diametral tensile strength and porosity.

Table 3.1 MCPM/β-TCP ratios for mechanical characterization

MCPM/β-TCP molar ratios	P/L ratios
1:1	1.00
	1.25
	1.50
1:3	1.00
	1.25
	1.50

Samples were prepared by measuring the powder components: MCPM (Strem Chemicals, New buryport, MA) and β-TCP (Fluka Chemical corporation, Ronkonkoma, NY). The MCPM and β-TCP powders were prepared according to the ratios in Table 3.1 using a balance (Mettler AE 100). The two powders were hand mixed in a mortar to ensure homogeneity. Deionized water was used as the liquid component. The powders and liquid of different P/L ratios were hand mixed by a metal spatula to ensure that the slurry was homogenous. After that, the slurry was casted into a cylindrical Telfon mold (5.90 mm diameter and 3.30 mm thickness). After allowing the cements paste to set for at least 30 minutes, the samples were removed from the molds. Then, the samples were dried in a vacuum desiccator chamber at room temperature for 48 hours.

Secondly, six groups of DCPD samples with MCPM/β-TCP = 1:1 were fabricated in two different shapes according to Table 3.2 with the same method as before to identify the better design of DCPD samples for further experiment.

Table 3.2 DCPD sample designs for mechanical characterization

Design	P/L ratios
Cylindrical shape (5.8 mm diameter and 4 mm thickness)	1.00
	1.25
	1.50
Disk shape (5 mm diameter and 2.5 mm thickness)	1.00
	1.25
	1.50

Finally, PLLA/DCPD composite samples were prepared. Three groups of DCPD disk samples with MCPM/β-TCP = 1:1 were fabricated in different powder to liquid ratios (1.00, 1.25 and 1.50) with the same method as above. After that, PLLA pellets were first dissolved in dichloromethane (CH_2Cl_2) solvent (1% and 5% w/w). Then, the DCPD disk samples were immersed into PLLA solution under vacuum to completely allow PLLA infiltration into the porous cement samples. In this experiment, nine groups of disk samples as shown in Table 3.3 were fabricated to investigate the fracture energy of samples.

Table 3.3 PLLA /DCPD composite samples for mechanical characterization

PLLA/DCPD composite disk samples	P/L ratios
Non-coating (control)	1.00
	1.25
	1.50
1% PLLA coating	1.00
	1.25
	1.50
5% PLLA coating	1.00
	1.25
	1.50

3.3 Experimental Procedure

3.3.1 Porosity of the DCPD Samples Before PLLA Coating

The porosity of the DCPD samples were calculated by the following equation:

$$\text{Porosity}\ (\%) = \left(1 - \frac{\rho_{Sample}}{\rho_{DCPD}}\right) \times 100 \quad (3.1)$$

which "ρ_{Sample}" is the bulk density and "ρ_{DCPD}" is the theoretical density of DCPD cements, which is 2.318 g/cm^3 [27]. Ten samples per group were measured in this experiment.

3.3.2 Diametral Tensile Strength and Fracture Energy

Mechanical properties of DCPD and PLLA/DCPD composite samples were evaluated using a universal material testing machine (MTS Systems, Eden Prarie, MN).

All samples were loaded at a rate of 1 mm/min. The compressive load was applied along a diametral plane of the cylinder, as shown in the Fig. 3.1, to determine failure load and fracture energy. Ten samples per group were measured for each test in this experiment.

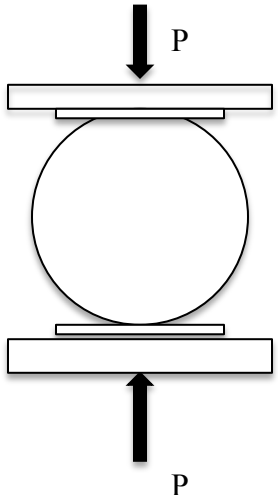

Figure 3.1 Diagram showing the compressive loads applied along two generators (diametral plane).

Diametral tensile strength σ_t (MPa) was calculated based on the failure load P (N) that applied to the samples during diametral compresstion test with this following equation:

$$\sigma_t = 2P/\pi DL \tag{3.2}$$

where D = diameter of samples (mm) and L = thickness of samples (mm) [41].

3.3.3 Statistical Analysis

Two-way analysis of variance (ANOVA) with the post hoc Tukey-Kramer multiple-range test was used to determine the significant differences of the effect of MCPM/β-TCP ratios and P/L ratios on the diametral tensile strength. A level of $\alpha = 0.05$

was used for statistical significance. In addition, the effect of P/L on cement porosity, the effect of geometry of samples on diametral tensile strength, and the effect of PLLA coating on the fracture energy were analyzed using an one-way ANOVA.

3.4 Results and Discussion

3.4.1 Porosity of DCPD Samples

It has been shown in several studies that diametral tensile strength of DCPD cements was strongly influenced by porosity[8, 27]. In this experiment, the powder to liquid (P/L) ratios were adjusted to control the porosity of the cylindrical DCPD samples. Increasing the P/L ratios yielded the higher porosity of the cements in the Fig. 3.2 and Fig. 3.3. Furthermore, it can be seen in Fig. 3.2 that when P/L ratio increased from 1.00 to 1.50, the porosity significantly decreased from $63.69 \pm 3.40\%$ to $55.15 \pm 2.86\%$ ($p < 0.05$). Similarly, Fig. 3.3 showed that increasing P/L ratio from 1.00 to 1.50, the porosity significantly decreased from $62.50 \pm 3.39\%$ to $53.60 \pm 5.10\%$ ($p < 0.05$). In addition, the highest porosities of both MCPM/β-TCP ratios were observed at the P/L = 1.00.

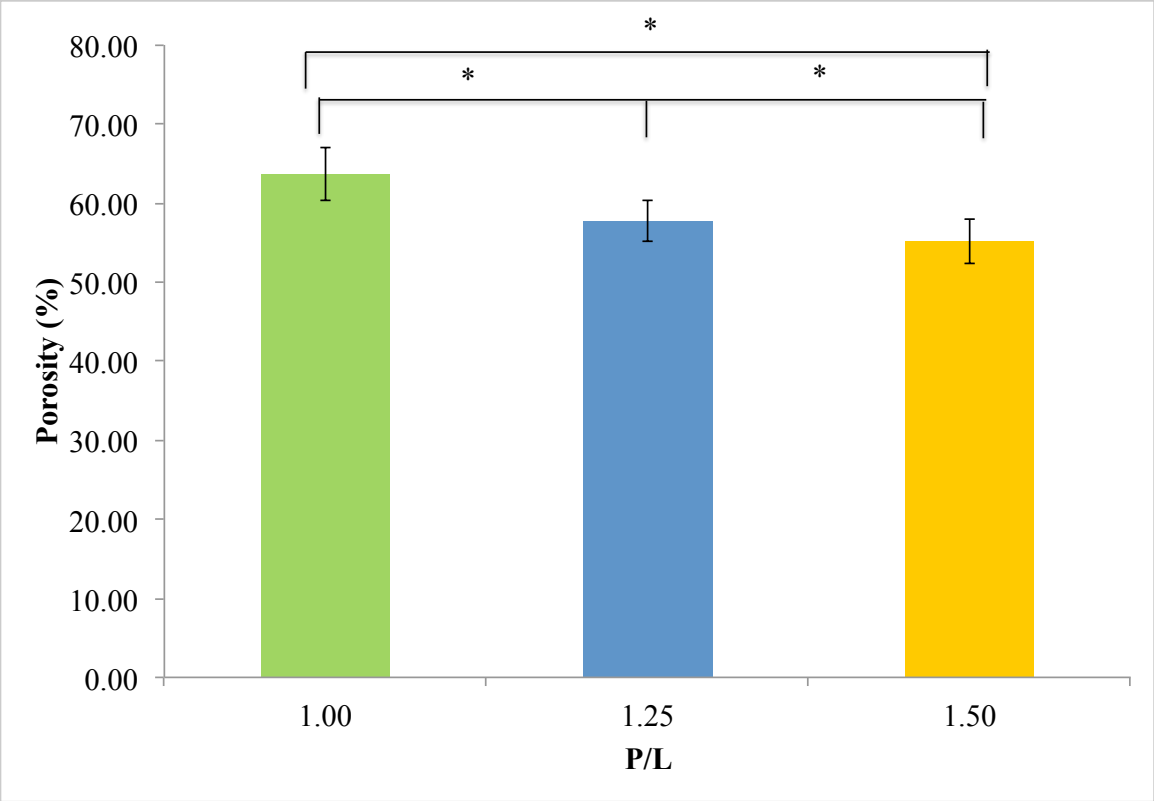

Figure 3.2 Porosity of cylindrical DCPD samples with MCPM/β-TCP = 1:3 at P/L = 1.00, 1.25 and 1.50. Marker indicates a significant difference ($p < 0.05$).

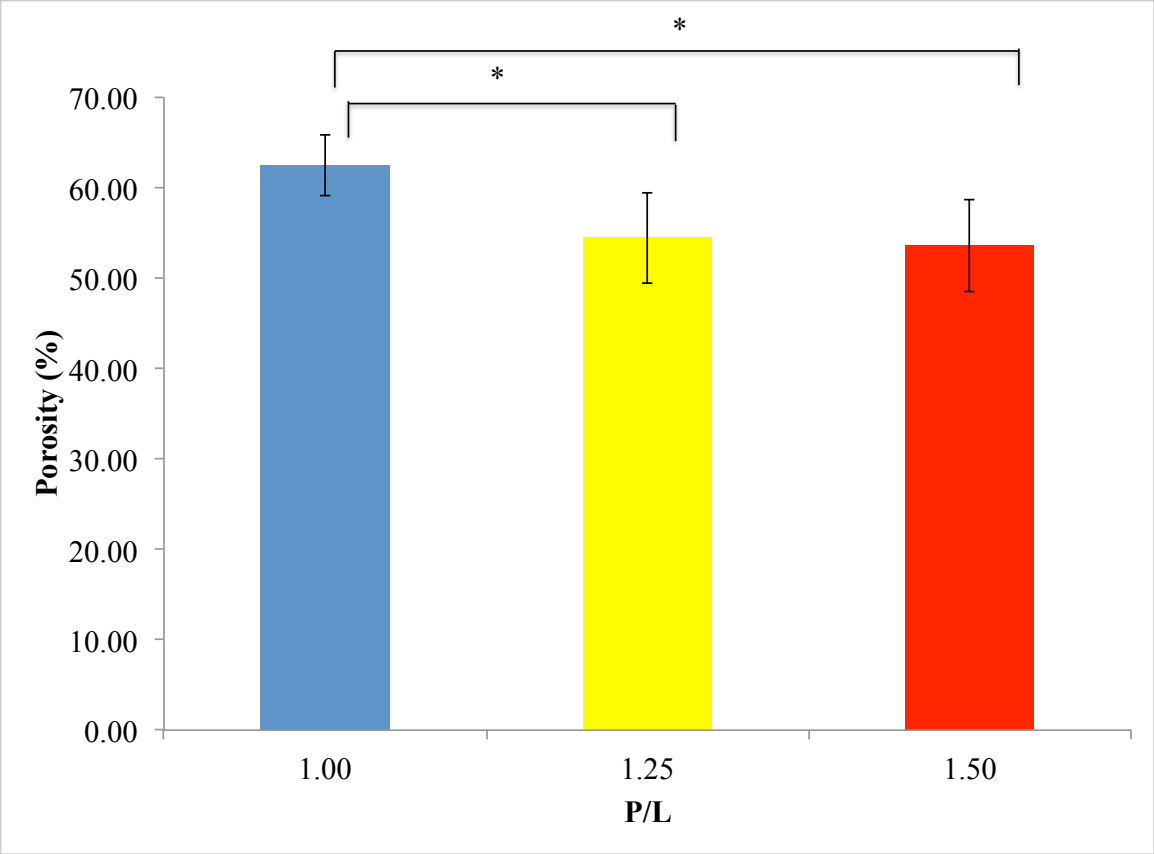

Figure 3.3 Porosity of cylindrical DCPD samples with MCPM/β-TCP = 1:1 at P/L = 1.00, 1.25 and 1.50. Marker indicates a significant difference ($p < 0.05$).

3.4.2 Diametral Tensile Strength Analysis

Porosity has a significant effect on the diametral tensile strength of calcium phosphate cements [24]. A diametral tensile strength is negative correlated to the porosity. In addition, a diametral tensile strength has inversely linear relationship with porosity followed a logarithmic trend (Fig. 3.4 and 3.5), which is the characteristic of Ryshkewitch relationship [42].

$$S = S_0 \exp(-bp) \tag{3.3}$$

$$lnS = lnS_0 - bp \tag{3.4}$$

where S is diametral tensile strength of porous samples, S_0 is the ideal diametral tensile strength at porosity equaled to zero, b is an empirical constant, and p is the percent porosity. The following models are developed based on the Fig. 3.4 and 3.5 respectively:

$$S = 29.441e^{-0.075p} \quad (3.5)$$

$$S = 110.42e^{-0.096p} \quad (3.6)$$

Based on the Equation 3.6 and Fig. 3.5 , the average of the ideal diametral tensile strength at zero porosity was estimated to be 110.42 MPa, which is higher than the diametral tensile strength (103 MPa) that was reported by Ishikawa and Asaoka [42].

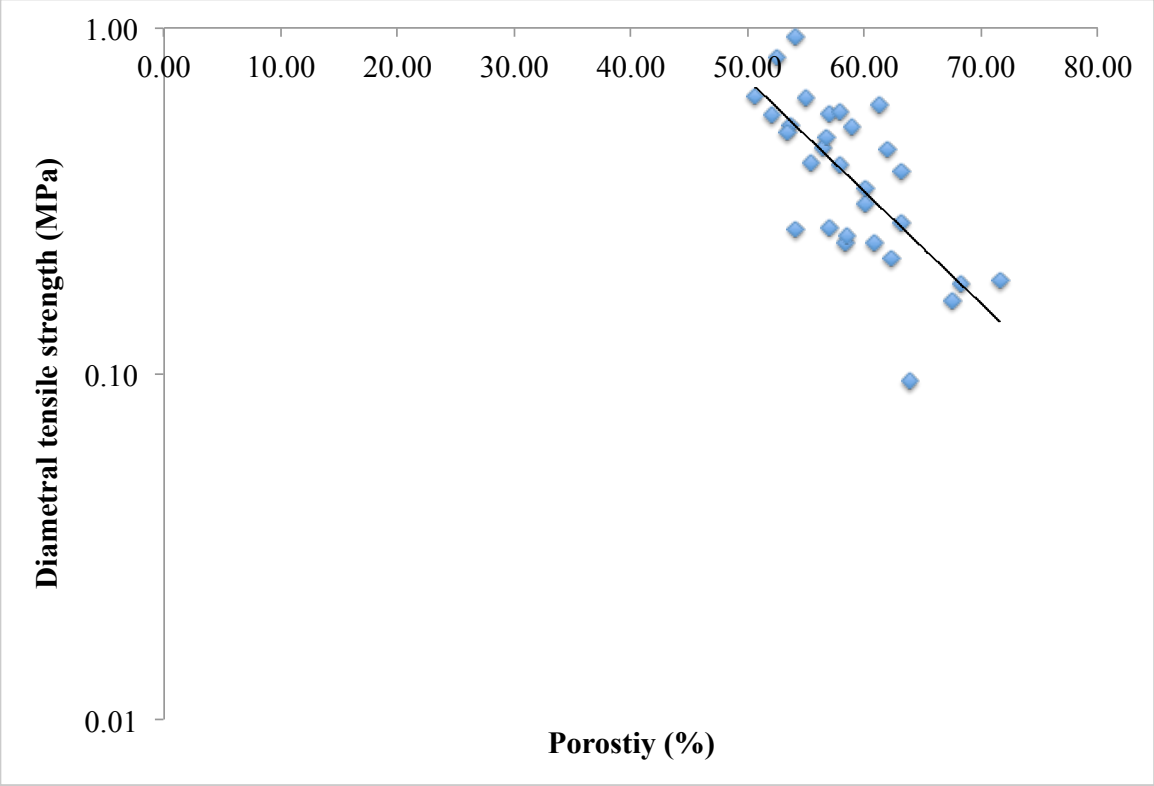

Figure 3.4 Relationship between the porosity and diametral tensile strength of cylindrical DCPD samples at MCPM/β-TCP = 1:3. Tensile strength versus percent porosity was plotted for individual samples. The data followed a logarithmic trend was modeled under the Ryshkewitch relationship ($S = 29.441e^{-0.075p}$, where S was diametral tensile strength of porous samples, and p was the porosity).

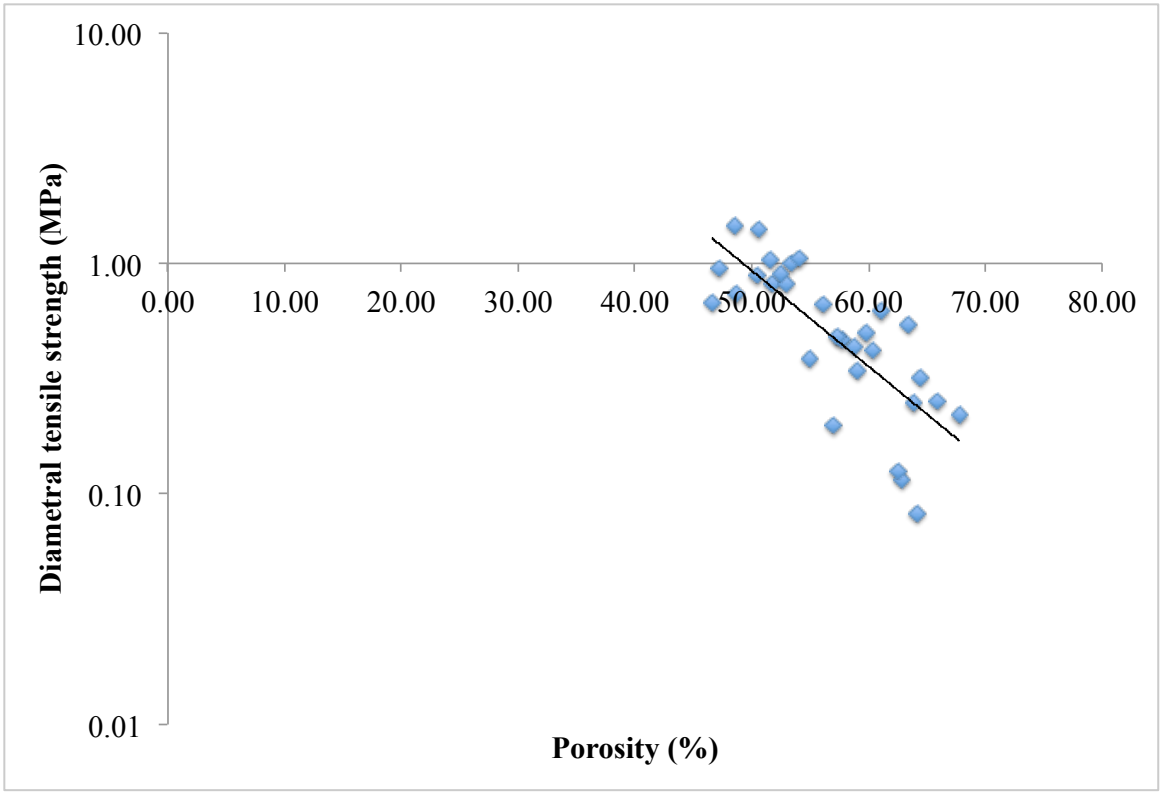

Figure 3.5 Relationship between the porosity and diametral tensile strength of cylindrical DCPD samples at MCPM/β-TCP = 1:1. Tensile strength versus porosity was plotted for individual samples. The data followed a logarithmic trend was modeled under the Ryshkewitch relationship ($S = 110.42e^{-0.096p}$, where S was diametral tensile strength of porous samples, and p was the porosity).

Fig. 3.6 indicated that the diametral tensile strength of cylindrical DCPD samples with MCPM/β-TCP ratio = 1:3 at P/L = 1.00, 1.25 and 1.50 were 0.28 ± 0.15, 0.42 ± 0.13, and 0.52 ± 0.22 MPa respectively. In addition, the diametral tensile strength of cylindrical DCPD samples with MCPM/-TCP ratio = 1:1 at P/L = 1.00, 1.25 and 1.50 were 0.34 ± 0.15, 0.65 ± 0.33, and 0.82 ± 0.42 MPa respectively.

The effect of MCPM/ β-TCPs and P/L ratios on diametral tensile strength was analyzed by two way Anova. Based on Fig. 3.6, the results demonstrated that the the diametral tensile strength of cylindrical DCPD samples at MCPM/ β-TCP = 1:1 were not significantly higher than the samples at MCPM/ β-TCP = 1:3. However, the diametral

tensile strength of the samples at P/L = 1.5 was significantly higher than the samples at P/L = 1.0 at MCPM/ β-TCPs = 1:3. In addition, the diametral tensile strength of the samples at P/L = 1.25 was also signifcicantly higher than the samples at P/L = 1.0 whie no significant different was found between the samples at P/L = 1.25 and 1.00.

The excess of β-TCP might be the cause of the lower diametral tensile strength of DCPD samples at MCPM/β-TCP = 1:3. When preparing DCPD from MCPM and β-TCP, DCPD was derived under a ceramic-ceramic composite, which was composed of the DCPD needle crystals and the remaining of unreacted β-TCP. The β-TCP component acted as the filler phase while the precipitated DCPD needles acted as the matrix or the phase that bound β-TCP component together. The excess of β-TCP component for deriving DCPD resulted in the higher unreacted β-TCP contents in DCPD composite, which leaded to a lower homogeneity of the cements. Therefore, the DCPD samples that contained lower homogeneity would yield lower tensile stregth [22].

As it can be seen in Fig. 3.6, the group of samples at MCPM/β-TCP = 1:1 at P/L = 1.00, 1.25 and 1.50 were chosen to be further investigated due to the higher diametral tensile strengths than the groups of MCPM: β-TCP = 1:3.

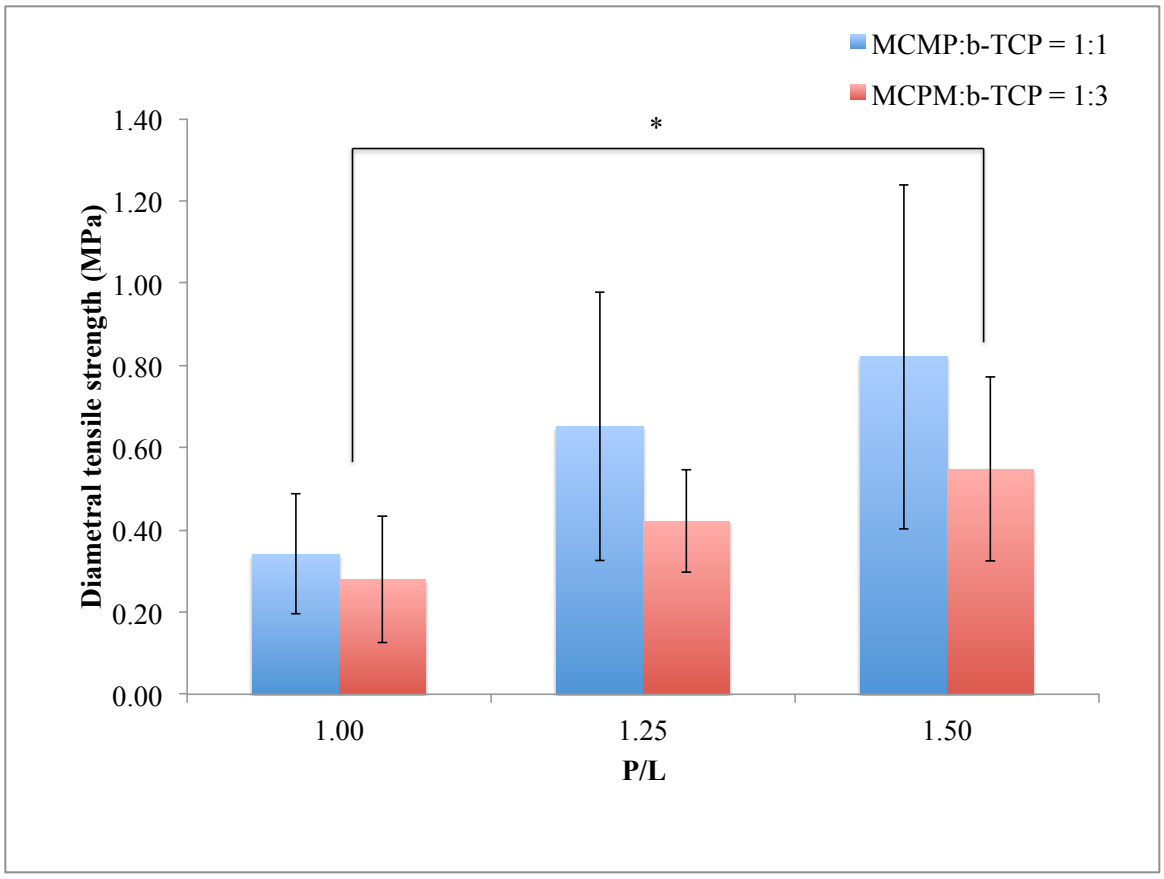

Figure 3.6 The effect of MCPM/ β-TCP ratios on diametral tensile strength of cylindrical DCPD samples.

3.4.3 The Effect of the Geometry of DCPD Samples on Diametral Tensile Strength

To study the effect of geometry of DCPD samples on diametral tensile strength, ten DCPD samples at MCPM/β-TCP = 1:1 for each design (disk and cylindrical) were fabricated and measured for the diametral tensile strength. Fig. 3.7 indicates that the diametral tensile strengths of cylindrical DCPD samples with MCPM/β-TCP ratio = 1:1 at P/L = 1.00, 1.25 and 1.50 were 0.40 ± 0.15, 0.71 ± 0.33, and 0.88 ± 0.42 MPa respectively. In addition, the diametral tensile strength of DCPD disk samples with MCPM/β-TCP ratio = 1:1 at P/L = 1.00, 1.25 and 1.50 were 0.14 ± 0.01, 0.18 ± 0.02, and 0.23 ± 0.04 MPa respectively.

As expected, the geometry of DCPD samples strongly affected on diametral tensile strength. In addition, at P/L = 1.25 and 1.50, the diametral tensile strength of cylindrical DCPD samples (0.71 ± 0.33 and 0.88 ± 0.42 MPa) were significantly higher than the diametral tensile strength of DCPD disk samples (0.01, 0.18 ± 0.02 and 0.23 ± 0.04 MPa) ($p < 0.05$). However, there was no significant difference was found between the diametral tensile strength of cylindrical DCPD samples and DCPD disk samples at P/L = 1.00.

Based on the Equation 3.2 ($\sigma_t = 2P/\pi DL$), the cylindrical DCPD samples absorbed higher failure load (P) than DCPD disk samples. However, the DCPD disk samples had smaller diameter (5 mm) and smaller thickness (2.5 mm) than the cylindrical DCPD samples (5.8 mm diameter and 4 mm thickness). The cylindrical DCPD samples yielded greater diametral tensile strength than disk samples due to the greater amount of failure load that were absorbed to the cylindrical DCPD,

As a result from Fig. 3.7, the group of DCPD disk samples at MCPM/ β-TCP = 1:1 were chosen for further experiment according to the smaller standard deviation of diametral tensile strength at all P/L ratios (1.00, 1.25 and 1.50). Although, this DCPD disk group of samples had lower diametral tensile strength, they were easier to control with smaller standard deviation.

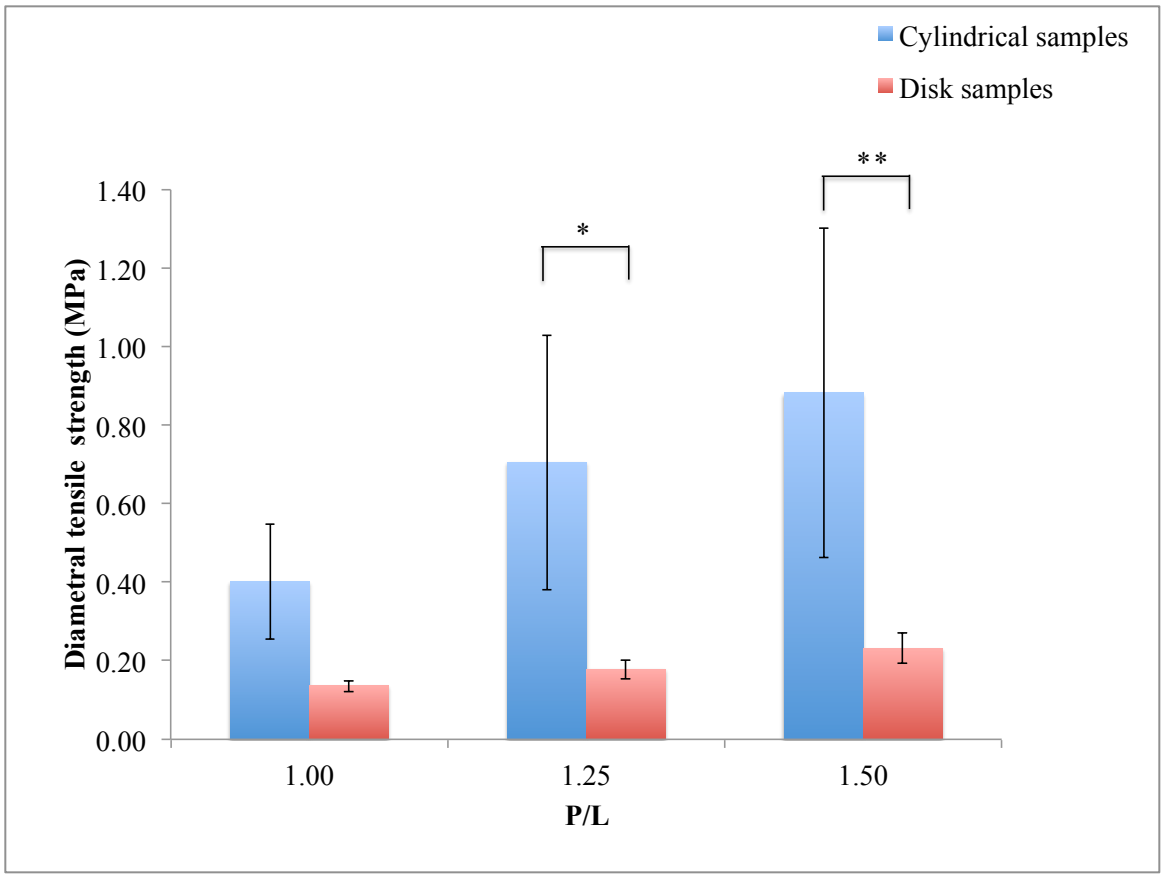

Figure 3.7 The effect on the geometry of DCPD samples at MCPM/β-TCP = 1:1 on diametral tensile strength. Marker indicates a significant difference ($p < 0.05$).

3.4.4 The Effect of PLLA Coating on the Fracture Energy

To study the effect of PLLA coating on the fracture energy of DCPD disk samples at MCPM/β-TCP = 1:1, the samples were frabricated and coated with a thin layer of PLLA (1% PLLA or 5% PLLA) and measured for the fracture energy. Fig. 3.8 indicates that at P/L 1.50, the fracture energy of the samples with 5% PLLA coating (3.9 $\pm$ 1.17 N-mm) was significantly higher than the control samples (1.35 $\pm$ 1.00 N-mm) ($p < 0.05$). However, there is no significant difference of fracture energy found within other P/L ratios (P/L = 1.00 and 1.25).

The fracture energy test shows that non-coating PLLA samples (control group) had lowest fracture energy at all P/L ratios. In addition, control samples were failed and

disintegrated due to their brittle property of the cement. However, the composite PLLA/DCPD samples retained the overall shape even though they were mechanically failed. Two groups of PLLA coated samples (1% and 5% w/w of PLLA) were showed to have higher fracture energy than control groups at all P/L ratios (1.00, 1.25 and 1.50). In addition, the fracture energy of 5% PLLA samples was significantly higher than control group at P/L = 1.50 ($p < 0.05$) indicating that PLLA matrix played an important role in improving the toughness of DCPD samples by binding the sample into a whole body. In addition, PLLA have been showed in improving the mechaincal properites of hydroxyapatite scaffolds through PLLA coating [43].

In general, the calcium phosphate cements scaffolds contain open micro cracks in the struts after dehydration. The thin layer of PLLA coating filled the pre-existing open micro pores and the exposed micro cracks on the surface of the scaffolds and formed an interlaced structure. PLLA coatng can improve the fracture energy of DCPD specimens because the polymer ligaments stretched upon the crack opening and energy consumption during the microcracks propagate to maintain the toughness of DCPD specimens by bridging the cracks. To further the experiment, the groups of DCPD samples coated with 5% PLLA at P/L = 1.00, 1.25 and 1.50 were chosen for further experiment due to the higher fracture energy.

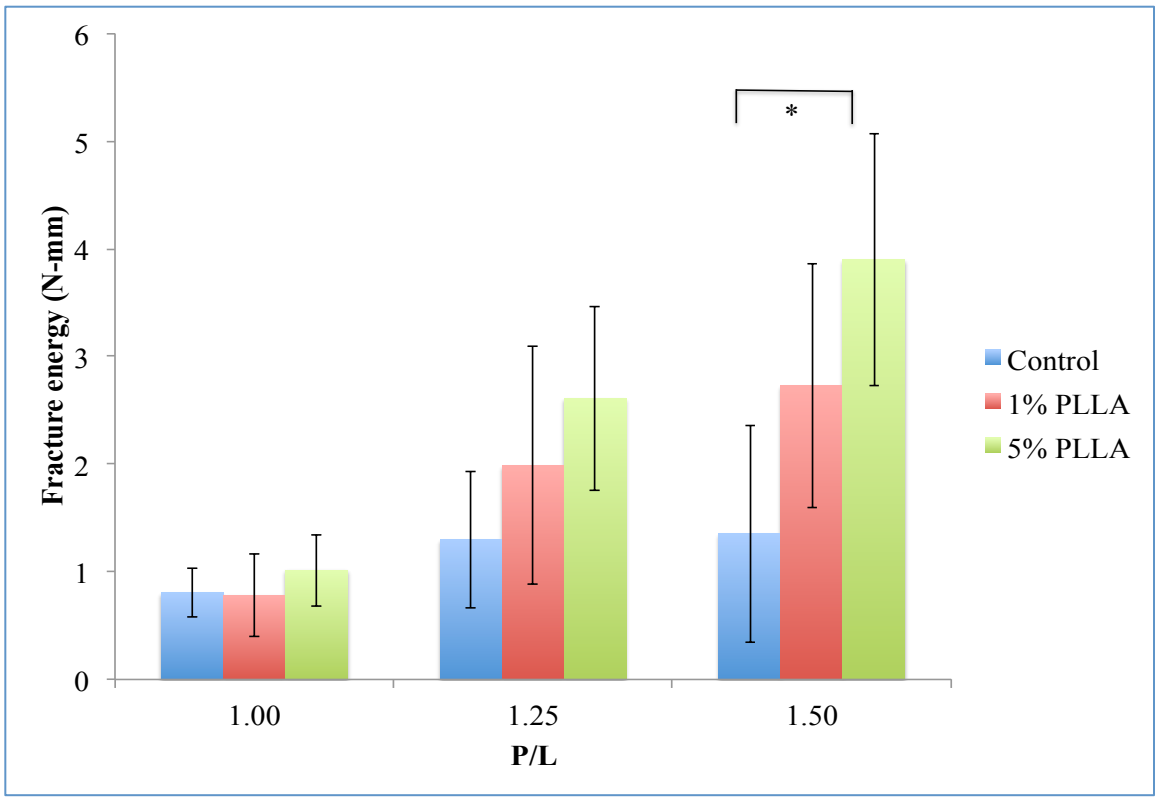

Figure 3.8 The effect of PLLA coating on the fracture energy of DCPD disk samples at MCPM/β-TCP = 1:1. Marker indicates a significant difference ($p < 0.05$).

4. EFFECT OF SODIUM CITRATE

4.1 Introduction

The purpose of this chapter was to study the effect of sodium citrate on the mechanical properties of the DCPD cements. In this chapter, the experiment was continued by fabricating DCPD and PLLA/DCPD samples with the chosen condition as mentioned in Chapter 3. DCPD and PLLA/DCPD disk samples were fabricated with MCPM: β-TCP = 1:1. In addition, 5% PLLA were coated on DCPD disk samples to fabricate the PLLA/DCPD composite samples. The samples were fabricated by using sodium citrate and deionized water as the liquid components to compare the mechanical properties of the DCPD and PLLA/DCPD composite samples.

4.2 Sample Preparation

To study the effect of sodium citrate on the mechanical properties of DCPD, six groups of DCPD samples were fabricated using MCPM (Strem Chemicals, New buryport, MA) and β-TCP (Fluka Chemical corperation, Ronkonkoma, NY) correlated to the ratio of MCPM to β-TCP = 1:1 at different powder to liquid ratios (P/L): 1.00, 1.25, and 1.50. In addition, the first three groups were prepared using deionized water as the liquid component at P/L 1.00, 1.25, and 1.50 respectively while another three groups were prepared using 100 mM sodium citrate as the liquid component at the same P/L ratios. Two powder components (MCPM and β-TCP) were measured corresponding to the molar ratios mentioned above by a balance (Mettler AE 100). The two powders were hand mixed in a mortar to ensure homogeneity. Then, the powders and liquid component were mixed at different P/L mentioned above by a metal spatula to ensure a homogenous slurry. After that, the slurry was casted into an aluminum mold to fabricate DCPD disk

samples (5 mm diameter and 2.5 mm thickness). After allowing the cements paste to set for 8 min, the samples were removed from the mold. Then, the samples were dried in vacuum desiccator chamber at room temperature for 48 h. After drying, the diameter and the thickness of the samples were measured by Mitutoyo analog calipers to a tolerance of 0.01 mm. Then, the weight of each sample was measured using the balance (Mettler AE 100).

For the composite DCPD/PLLA samples preparation, six groups of DCPD disk samples mentioned above were fabricated. After drying, the diameter and the thickness of the samples were measured by Mitutoyo analog calipers to a tolerance of 0.01 mm. Then, the weight of each fully dried sample was measured using a balance (Mettler AE 100). Next, PLLA pellets were first dissolved in chloroform ($CHCl_3$) solvent (1% and 5%). After that, the DCPD disk samples were immersed into PLLA solution to completely allow PLLA infiltration into the porous cement samples. Then, the samples were dried under vacuum in desiccator chamber for 48 h. Finally, the samples were taken out to measure the weight using the balance prior to test the mechanical properties.

In this experiment, 10 samples of disk samples with regarded to Table 5.1 were fabricated to investigate the porosity, diametral tensile strength, and fracture energy of the samples.

Table 5.1 Twelve groups of samples for mechanical characterization

Group	Liquid phase	P/L	PLLA
1	Deionized water	1.00	Uncoated PLLA
2	Deionized water	1.00	Coated 5% PLLA
3	Deionized water	1.25	Uncoated PLLA
4	Deionized water	1.25	Coated 5% PLLA
5	Deionized water	1.50	Uncoated PLLA
6	Deionized water	1.50	Coated 5% PLLA
7	Sodium Citrate	1.00	Uncoated PLLA
8	Sodium Citrate	1.00	Coated 5% PLLA
9	Sodium Citrate	1.25	Uncoated PLLA
10	Sodium Citrate	1.25	Coated 5% PLLA
11	Sodium Citrate	1.50	Uncoated PLLA
12	Sodium Citrate	1.50	Coated 5% PLLA

4.3 Experimental Procedure

4.3.1 Porosity of the DCPD Samples

The porosity of the DCPD samples were calculated by the following equation:

$$\text{Porosity (\%)} = \left(1 - \frac{\rho_{Sample}}{\rho_{DCPD}}\right) \times 100 \quad (3.1)$$

where "ρ_{Sample}" is the bulk density and "ρ_{DCPD}" is the theoretical density of DCPD cement, which is 2.318 g/cm^3 [27]. Ten samples of each group in the Table 5.1 were fabricated to measure the porosity.

4.3.2 Diametral Tensile Strength and Fracture Energy

Mechanical properties of DCPD and PLLA/DCPD composite samples were evaluated on a universal materials testing machine (MTS Systems, Eden Prarie, MN). All samples were loaded at a rate of 1mm/min. The compressive load was applied along the diametral plane of the cylinder, as shown in Fig. 3.1, to determine failure load and fracture energy. Diametral tensile strength was calculated based on Equation 3.2. Ten samples per group were measured for each test in this experiment.

4.3.3 Statistical Analysis

Thee-way and one-way analysis of variance (ANOVA) with the post hoc Tukey-Kramer multiple-range test were used to determine the significant differences of the porosity and the effect of sodium citrate and PLLA coating on the diametral tensile strength and the fracture energy. A level of $\alpha = 0.05$ was used for statistical significance.

4.4 Results and Discussion

4.4.1 The Porosity

Several studies have reported that the diametral tensile strength of DCPD cements was strongly influenced by porosity [8, 39]. The powder to liquid ratios were used to adjust the porosity. Increasing powder to liquid ratios resulted in the reduction of the porosity as illustrated in Fig. 4.1 and 4.2. Fig. 4.1 indicated that the porosity of the deionized water group at P/L 1.50 (53.57% $\pm$ 2.56%) was siginificantly lower than P/L 1.25 group (57.44 $\pm$ 2.13%) and P/L 1.00 group (58.98 $\pm$ 2.36%) ($p < 0.05$). Fig. 4.2 illustrated that the porosity of the sodium citrate group at P/L 1.00 (59.33% $\pm$ 1.57%) was siginificantly higher than the groups at P/L 1.25 (58.82 $\pm$ 2.57%) and P/L 1.50 (53.19 $\pm$ 3.66%) ($p < 0.05$). However, in this experiment only the porosity of the DCPD samples was studied. The porosity of PLLA/DCPD samples will be studied in the future.

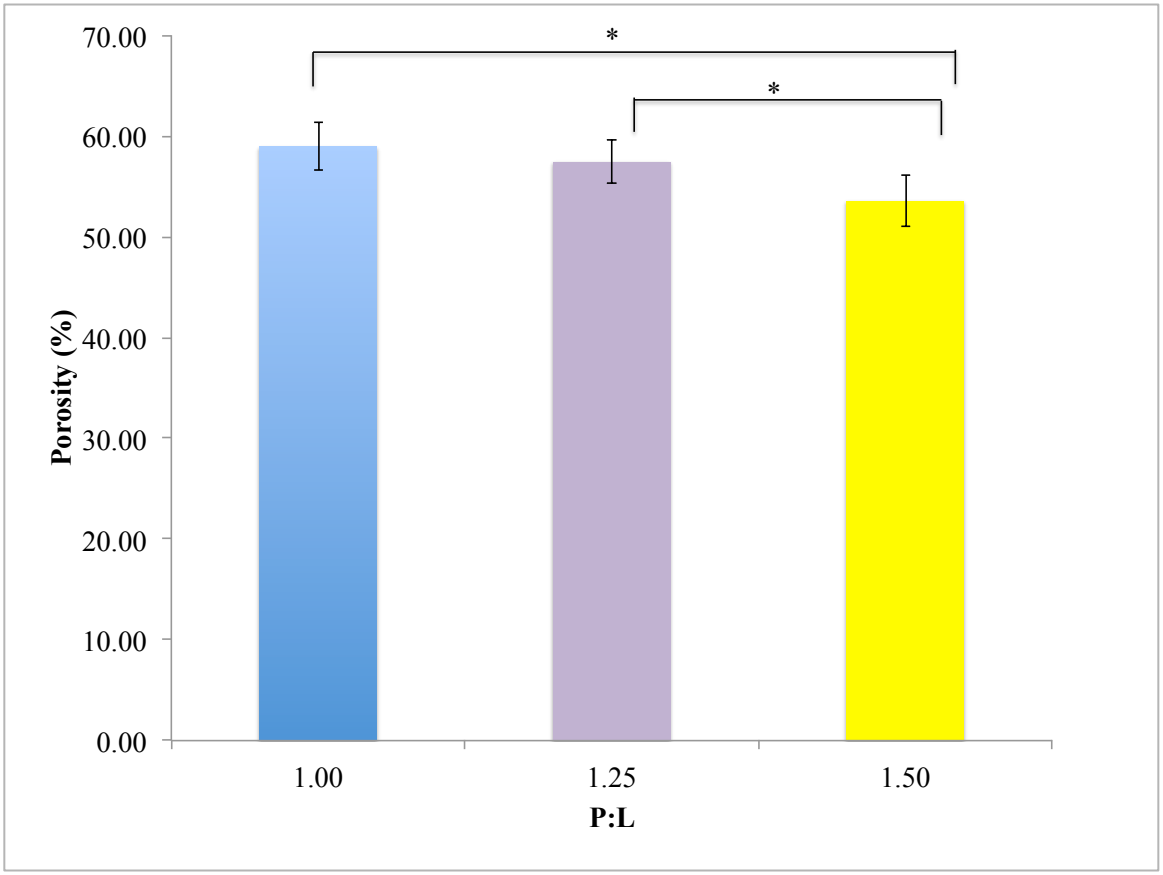

Figure 4.1 Porosity of DCPD samples (Dionized Water, 0% PLLA) at different P/L ratios : 1.00, 1.25, and 1.50. Marker indicates a significant difference ($p < 0.05$).

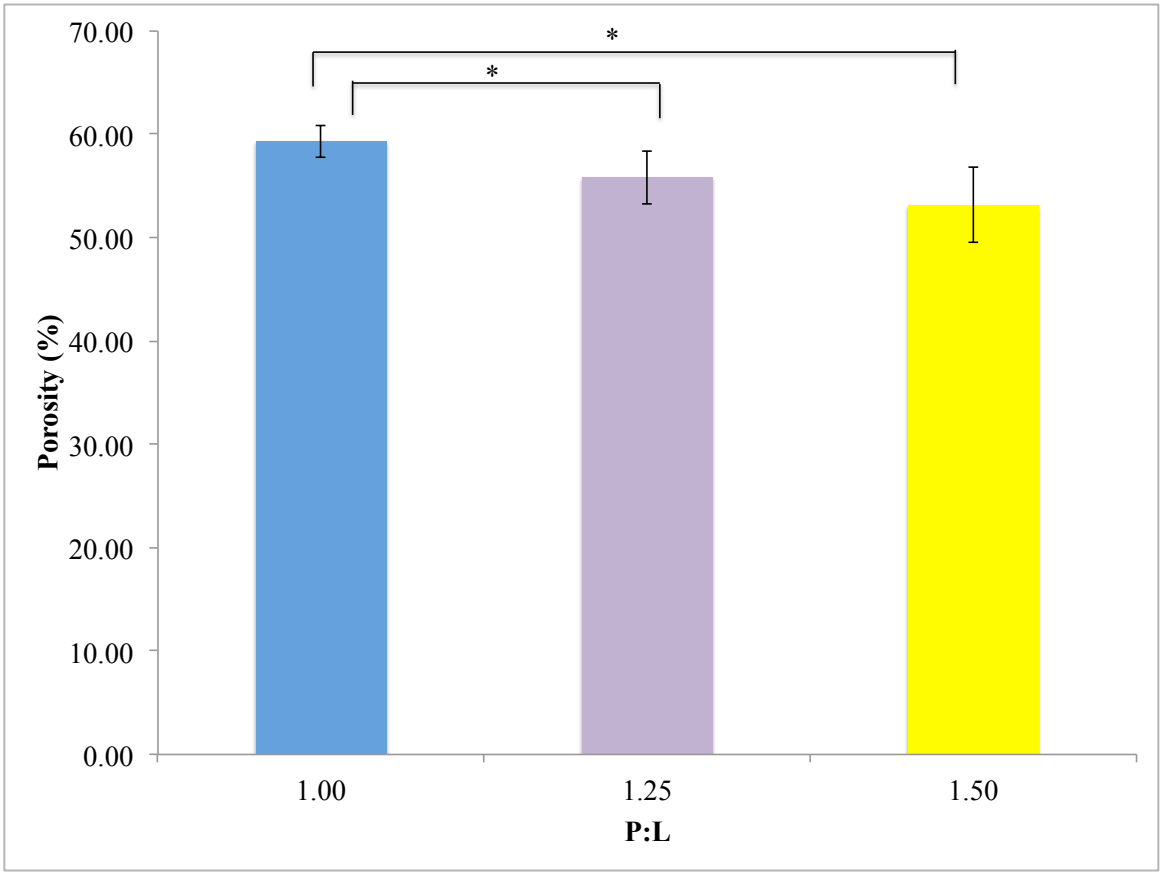

Figure 4.2 Porosity of DCPD samples (Sodium Citrate, 0% PLLA) at different P/L ratios : 1.00, 1.25, and 1.50. Marker indicates a significant difference ($p < 0.05$).

4.4.2 Diametral Tensile Strength Characterization

To study the effect of sodium citrate, ten samples of each group in Table 5.1 were fabricated and determined the diametral tensile strength. From three-way ANOVA, sodium citrate had a significant effect on the diametral tensile strength ($p < 0.05$). The diametral tensile strength of the samples with sodium citrate was significant higher than those samples with deionized water ($p < 0.05$). In addition, PLLA coating and P/L ratios also had significant effects on the diametral tensile strength. From one-way ANOVA, the the results in the Fig. 4.3 indicated the effect of sodium citrate and PLLA coating on diametral tensile strength of DCPD specimens. The sodium citrate significantly improved the diametral tensile strength of the specimens at all P/L molar ratios. The greatest improvement was found at P/L 1.50. The compressive strength of DCPD specimens improved from 1.05 ± 0.37 MPa to 1.87 ± 0.27 MPa. The significant effect of PLLA coating was showed at all P/L molar ratios for the DCPD specimens preparing from sodium citrate. However, the significant effect of PLLA coating was only indicated at P/L 1.25 for DCPD specimens preparing from deionized water. The highest diametral tensile strength of PLLA/DCPD composite specimens was 1.36 ± 0.22 MPa.

Fig. 4.3 indicates that the P/L ratios, PLLA coating, sodium citrate have significant effects on the diamentral tensile strength. The main reason was suggested that the diametral tensile strength was found to be related to the porosity of the cement samples. Reducing porosity by increasing P/L ratios resulted in the higher mechanical strength [8]. In the diametral compression test, the DCPD samples failed and disintegrated due to the brittle fracture of the struts. On the other hand, the composite PLLA/DCPD samples still retained the overall shape even though they were suffered from mechanical failure. Therefore, PLLA coating played an important role in improving mechanical properties of the samples by binding the samples into a whole piece. In addtion, the load was applied on the diametral plane as mentioned in Fig. 3.1 so the tensile strength was affect on the side of the specimens during diametral compression test. As PLLA bridging all DCPD specimen together as a whole piece, the tensile strength was maintained by the brigding of PLLA on the side of the specimen. Sodium

citrate was also a crucial key to improve mechanical properties of DCPD cements because sodium citrate would retard crystal growth resulted in the increase in cement compaction due to the reduction of the average crystal size [23].

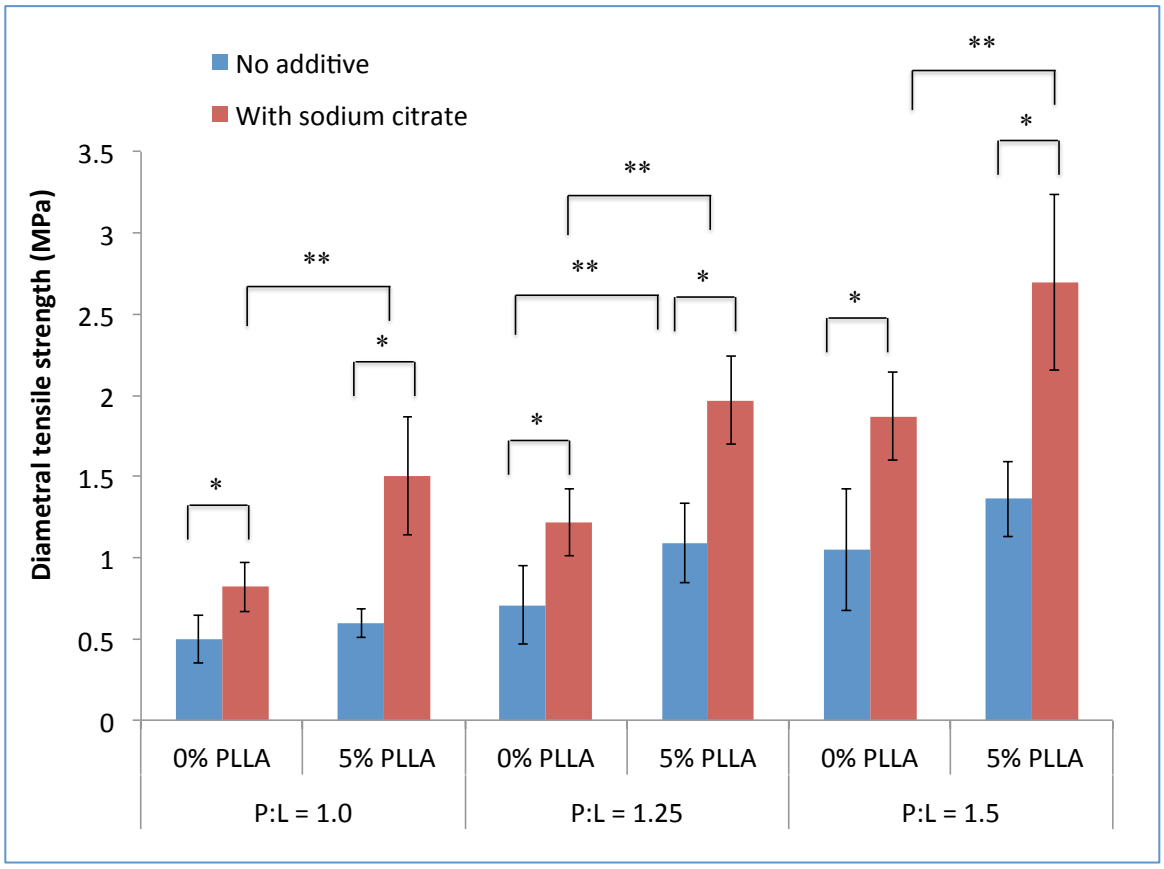

Figure 4.3 The effect of sodium citrate on diametral tensile strength of DCPD and PLLA/DCPD composite samples. (Signifcant different within each P/L molar ratio compared between two liquid phase and % PLLA coating are indicated by * and ** respectively. ($n = 10$; $p < 0.05$).

4.4.3 Fracture Energy Characterization

To study the effect of sodium citrate by characterizing the fracture energy of the samples, ten samples of each group in Table 5.1 were fabricated and determined the fracture energy. From three-way ANOVA, sodium citrate, P/L ratios, PLLA coating had significant effects on the fracture energy ($p < 0.05$). The fracture energy of the sodium citrate groups was significantly higher than the groups with deionized water ($p < 0.05$). In

addition, the fracture energy of P/L 1.50 groups were significantly higher than P/L 1.25 and 1.00 groups ($p < 0.05$). From one-way ANOVA, the result in the Fig. 4.4 indicated the effect of sodium citrate and PLLA coating on fracture energy of DCPD specimens. Using sodium citrate as the setting regulator improved the fracture energy of the specimens at all P/L ratios. The greatest improvement fracture energy was found at P/L 1.50 and the fracture energy increased from 2.53 ± 1.62 MPa to 6.31 ± 1.05 N-mm. The significant effect of PLLA coating was showed at all P/L ratios of the specimens preparing from sodium citrate. However, only one significant difference was found on the specimens preparing from deionized water at P/L 1.25. The highest fracture energy of PLLA/DCPD composite specimens was 12.67 ± 4.97 N-mm.

As mentioned before, the sodium citrate, PLLA, and P/L ratios had the significant effects on the fracture energy. The fracture energy was calculated from the area under the curve plotted between the load (N) and the displacement (mm). The addition of sodium citrate, PLLA coating, and increasing P/L ratios resulted in the increasig of the uder curve area and the higher of fracture energy. As mentioned before, the addition of sodium citrate resulted in smaller size of the crystals formed and more compaction of the cements, leading to the higher under curve area and fracture energy. Increasing the P/L ratios resulted in the lower porosity, the higher under curve area, and fracture energy. In addition, PLLA coating also increased the fracture energy with the higher under curve area due to binding the samples as a whole piece. The difference of the shape of the curves bettween 0% PLLA and 5% PLLA group were illustrated in the Fig. 4.3. In general, the calcium phosphate cements scaffolds contain open micro cracks in the struts after dehydration. The thin layer of PLLA coating filled the pre-existing open micro pores and the exposed micro cracks on the surface of the scaffolds and formed an interlaced structure. From the load-displacement curve of PLLA/DCPD composite Fig. 4.4, the load was sharply increased before steep drop and then a small plateau was demonstrated. The small plateau was considered as yield resistance increase after coating. In this research, the stretch PLLA fibril suggested the toughness of the composite scaffolds. According to Pezzotti and Asmus [44], the polymer ligaments stretched upon

the crack opening and energy consumption during the microcracks propagate to maintain the tougness of DCPD specimens.

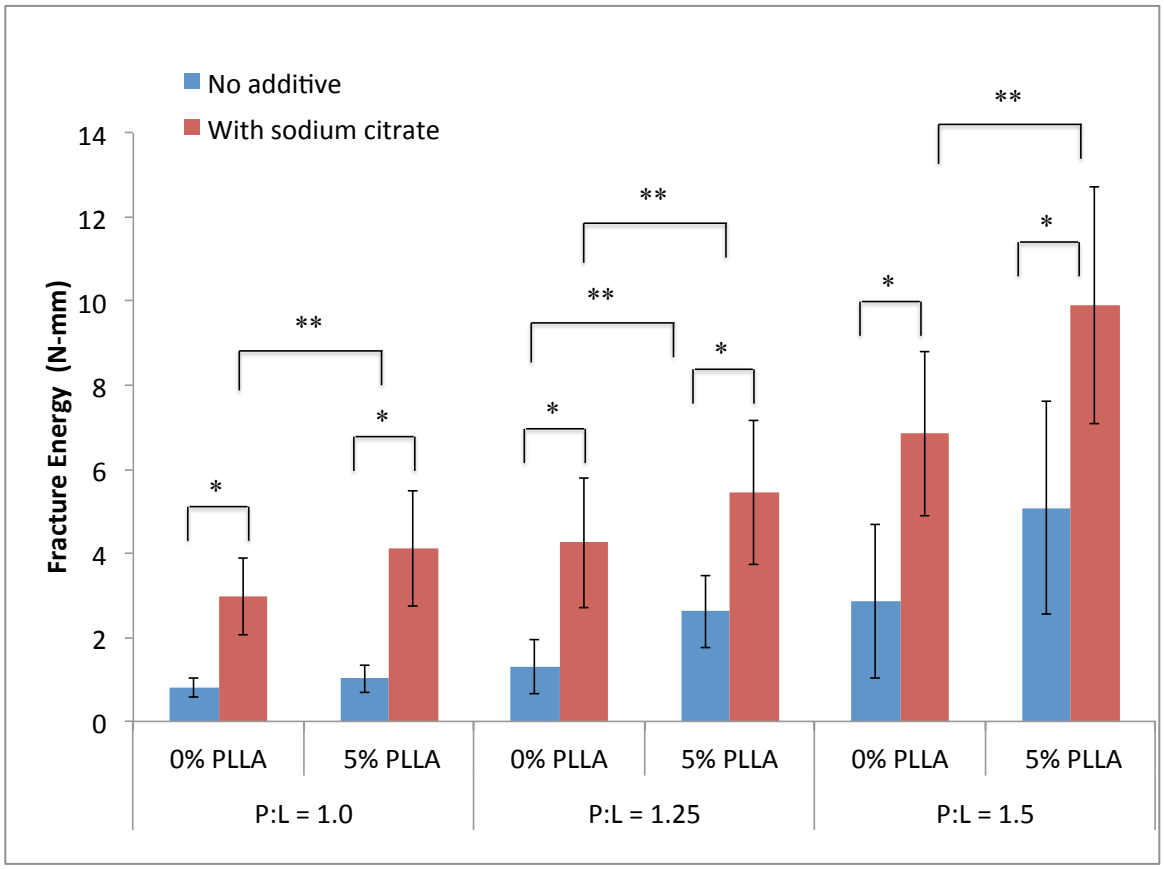

Figure 4.4 The effect of sodium citrate on fracture energy of DCPD and PLLA/DCPD composite samples. (Signifcant different within each P/L molar ratio compared between two liquid phase and % PLLA coating are indicated by * and ** respectively. (n = 10; $p < 0.05$).

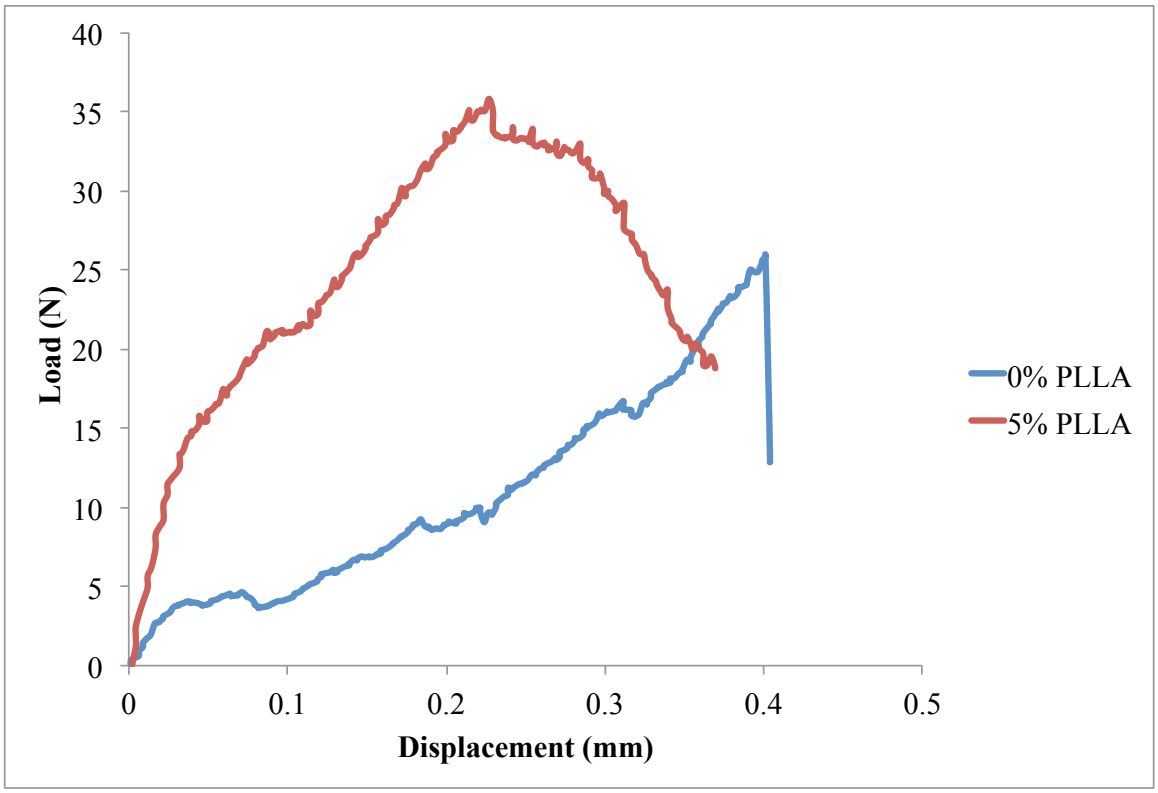

Figure 4.5 Representative load-displacement curve obtained during dimetral compression tests performed on the DCPD samples (Deionized water, P/L = 1.50) : 0 % PLLA and 5% PLLA. The fracture energy of 0% PLLA and 5% PLLA were 4.24 and 9.08 (N-mm), respectively.

5. IN VITRO DEGRDATION ANALYSIS

5.1 Introduction

Several studies have reported apatite cements more than brushite cements due to their better mechanical properties and the setting ability at neutral pH. However, an increasing of the attraction of brushite cement is initiated from their metastability under physiological conditions and an ability to resorb in vivo [32].

In this experiment dicalcium phosphate dehydrate (DCPD) degradation was researched by soaking in phosphate-buffered salt solution (PBS). DCPD cements fabricated with sodium citrate added to the liquid phase were also studied to investigate the influence of sodium citrate on brushite cement degradation. In addition, the PLLA was coated on the DCPD samples to investigate the effect of coating during in vitro degradation.

To study the in vitro degradation of DCPD and PLLA/DCPD samples, the properties, such as pH, mass loss, and energy to fracture were measured during in vitro degradation to determine the structural changes during the degradation. The following sections will describe the sample preparation and the experiment procedure of samples aged by static and dynamic degradation in PBS.

5.2 Sample Preparation

To study the static degradation in PBS, twelve groups of DCPD samples were fabricated using MCPM (Strem Chemicals, New Buryport, MA) and β-TCP (Fluka Chemical, Ronkonkoma, NY) correlated to the molar ratio of MCPM to β-TCP = 1:1 at

different powder to liquid ratios (P/L): 1.00, 1.25, and 1.50. In this experiment, first three groups were fabricated at different P/L as mentioned above using deionized water as the liquid component. In addition, 100 mM sodium citrate solution was used as the liquid component for the other three groups. Two powder components (MCPM and β-TCP) were measured corresponded to the molar ratios mentioned above with a balance (Mettler AE 100). The two powders were hand mixed in a mortar to ensure homogeneity. Then, the powders and liquid component were mixed at different P/L mentioned above by a metal spatula to ensure a homogenous slurry. After that, the slurry was casted into an aluminum mold to form DCPD disk samples (5 mm diameter and 2.5 mm thickness). After allowing the cement paste to set for 8 min, the samples were removed from the mold. Then, the samples were dried in a vacuum desiccator chamber at room temperature for 48 h. After that, the samples were taken out and measured the weight by the balance. For the composite DCPD/PLLA samples, six groups of DCPD disk samples mentioned above were fabricated. After that, PLLA pellets were dissolved in chloroform ($CHCl_3$) solvent (5 %). Then, the DCPD disk samples were immersed into PLLA solution under chemical hood. Then, the samples were taken out and dried in vacuum desiccator chamber at room temperature for 48 h. Then, the weight of the fully dried samples was measured using the balance. In this experiment, twelve groups of DCPD disk samples were fabricated according to the Table 5.1. The percentage of weight loss, pH changes, and fracture energy was determined during this static degradation study.

Table 5.1 Twelve groups of samples for static degradation testing

Group	Liquid phase	P/L	PLLA
1	Deionized water	1.00	Uncoated PLLA
2	Deionized water	1.00	Coated 5% PLLA
3	Deionized water	1.25	Uncoated PLLA
4	Deionized water	1.25	Coated 5% PLLA
5	Deionized water	1.50	Uncoated PLLA
6	Deionized water	1.50	Coated 5% PLLA
7	Sodium citrate	1.00	Uncoated PLLA
8	Sodium citrate	1.00	Coated 5% PLLA
9	Sodium citrate	1.25	Uncoated PLLA
10	Sodium citrate	1.25	Coated 5% PLLA
11	Sodium citrate	1.50	Uncoated PLLA
12	Sodium citrate	1.50	Coated 5% PLLA

To study the dynamic degradation in PBS, four groups of DCPD and PLLA/DCPD composite samples mentioned in Table 5.2 were chosen for dynamic PBS degradation. The percentage of weight loss, pH changes, and fracture energy was determined during this static degradation study.

Table 5.2 Four groups of samples for dynamic degradation testing

Group	Liquid phase	P/L	PLLA
1	Deionized water	1.50	Uncoated PLLA
2		1.50	Coated 5% PLLA
3	Sodium citrate	1.50	Uncoated PLLA
4		1.50	Coated 5% PLLA

5.3. Experimental Procedure

5.3.1 In Vitro Static Degradation in PBS

Twenty samples of each experimental group as in Table 5.1 were prepared for the static degradation test. The samples were placed individually in a glass vial containing 3 ml of PBS at pH 7.4 and incubated at 37℃ for up to 42 days with no soaking media changes. Five samples from each group were removed from the incubator at 1, 7, 28, and 42 days. Then, samples were dried under vacuum in the desiccator chamber for 48 h and weighted to determine the percent of weight loss during degradation.

5.3.2 In Vitro Dynamic Degradation in PBS

Thirty-six samples of each experimental group as in the Table 5.1 were prepared for the dynamic degradation test. The samples were placed individually in a glass vial containing 3 ml of PBS at pH 7.4 and incubated at 37℃ for up to 56 days. In addition, the soaking media was changed every 14 days. Six samples from each group were removed from the incubator at 1, 7, 14, 28, 42, and 56 days. Then, the samples were dried under vacuum in the desiccator chamber for 48 h. After that five samples from each group were weighted to determine the percent of weight loss during degradation. Moreover, one sample of each group at different time points was taken to observe the surface morphology by a scanning electron microscope (SEM, JEOL JSM-5310LV).

5.3.3 Mass Loss Testing

The fully dried samples were weighed to determine the percentage of weight loss during degradation. The percentage of weight loss were calculated with the following equation:

$$\text{Percentage of weight loss (WL \%)} = \frac{W_0 - W_d}{W_0} \times 100 \quad (5.1)$$

where W_0 represents the initial weight of the samples before soaking in PBS and W_d denotes the weight of the dried samples after degradation at different time periods [45].

5.3.4 pH Testing

The pH of the PBS in the each glass vial after removing a sample was measured with a pH meter (Denver Instruments, Arvada, CO), which was calibrated with the buffer solutions prior to use each time.

5.3.5 Fracture Energy Testing

Fracture energy of each fully dried sample after soaking in PBS at different time points was evaluated using a universal materials testing machine (MTS Systems, Eden Prarie, MN). All samples were loaded at a rate of 1mm/min. The compressive load was applied along a diametral plane of the samples, as demonstrated before in the Fig. 3.1. For both static and dynamic degradation study, five samples from each experimental group were measured for each test in this experiment.

5.3.6 SEM Analysis

The surface morphology of the samples was investigated by a scanning electron microscope (SEM, JEOL JSM-5310LV). One fully dried sample from each experimental group at different time points was sputter coated with gold for SEM analysis.

5.3.7 Statistic Analysis

Quantitative data for weight loss and pH were presented in the form of ± the standard deviation. One-way analysis of variance (ANOVA) with the post hoc Tukey-Kramer multiple-range test was used to determine the significant differences between experimental groups. A level of $\alpha = 0.05$ was used for statistical significance.

5.4 Results and Discussion

5.4.1 In Vitro Static Degradation

The percentage of weight loss (WL %) of DCPD and PLLA/DCPD compostie samples (without sodium citrate additive) as a function of immersion time was shown in Fig. 5.1. After immersion in PBS solution for 7 days, the P/L :1.00 and 1.50 with 0% PLLA groups had lost 3.55 $\pm$ 1.47% and 3.78 $\pm$ 0.49 % of their masses, respectivetly. In addtion the P/L 1.00 (5% PLLA), P/L 1.25 (0% PLLA), P/L 1.25 (5% PLLA), and P/L 1.50 (5%) PLLA groups lost 2.29 $\pm$ 0.41 %, 1.92 $\pm$ 0.14 %, 2.44 $\pm$ 1.39 %, and 2.41 $\pm$ 0.59 % of their masses, respectively. After day 7, the WL percentage of DCPD and PLLA/DCPD samples tended to stablize. Then, the DCPD and PLLA/DCPD composite samples started to degrade again after day 28. The final percentage of weight loss on day 42 of P/L 1.00 (0% PLLA), P/L 1.00 (5% PLLA), P/L 1.25 (0% PLLA), P/L 1.25 (5% PLLA), P/L 1.50 (0%), and P/L 1.50 (5%) groups were 6.57 $\pm$ 2.64 %, 5.03 $\pm$ 0.72 %, 5.94 $\pm$ 1.01 %, 4.69 $\pm$ 1.42 %, 4.83 $\pm$ 1.62 %, and 3.67 $\pm$ 0.75 %, respectiviely. The percentage of weight loss between 0% PLLA and 5% PLLA of each P/L ratio were not significant different at each time point ($p > 0.05$). However, The difference of percentage of weight loss between 0% PLLA and 5% PLLA tended to be the largest at P/L = 1.50.

As mentioned in Chapter 2, the 3 in vitro DCPD degradation mechanisms were dissolution, disintegration, and conversion [31]. Dissolution started when the samples were placed in solution with undersaturated calcium and phosphate ions resulted in mass loss during day 1. The high degree of dissolution lead to the cements disintegration causing an increase of mass loss after day 1. After 7 days, the solubility limit was reached and the solution became saturated. Therefore, the percent weight loss of the samples tended to be stabilized during day 7 to day 28. Since DCPD was mestastable at pH > 4, the solution became supersaturated. As a results, DCPD was converted to HA leading to further mass loss of DCPD after day 28 similar to the studies of Alge et al. [31].

The percentage of weight loss (WL %) of DCPD and PLLA/DCPD composite samples (with sodium citrate additive) as a function of immersion time was shown in Fig. 5.2. After immersion in PBS solution for 1 day, the P/L 1.00 (5% PLLA), P/L 1.25 (0% PLLA), P/L 1.25 (5% PLLA), and P/L 1.50 (5%) PLLA groups lost 5.40 ± 0.35 %, 3.83 ± 1.00 %, 4.46 ± 0.20 %, 3.99 ± 0.43 %, 4.43 ± 0.70 %, and 3.96 ± 0.44 % of their masses, respectively. After that, the percentage of weight loss tended to stabilize. The percentage of weight loss between 0% PLLA and 5% PLLA of each P/L ratio were not significant different at each time point ($p > 0.05$). However, the difference of percentage of weight loss between 0% PLLA and 5% PLLA tended to be hightest at P/L = 1.50.

The dissolution of DCPD cements start when the samples were placed into the PBS solution. The high dissolution of DCPD leaded to the disintegradation of cements and an increase of mass loss during the first day of immersion. Then, the solution was saturated and the weight loss became stabilized. During first week, the degradation of DCPD and PLLA/DCPD samples with sodium citrate tended to degrade faster in PBS than the samples without sodium citrate additive because sodium citrate was used as a setting regulator to inhibit the growth of DCPD crystals formation resulting in small DCPD crystals and leading to more interfacial area between DCPD crystals (without sodium citrate additive) and PBS [8]. As a result, the DCPD and PLLA/DCPD samples were degraded faster than the samples without sodium citrate additive. In addition, the PBS solution tended to be saturated after day 1 while the PBS solution of the other samples (without sodium citrate additive) tended to be saturated after day 7.

It is interesting to notice that the results suggest that citrate additive to have a stronger effect on the dissolution behaviors of DCPD than the PLLA coating.

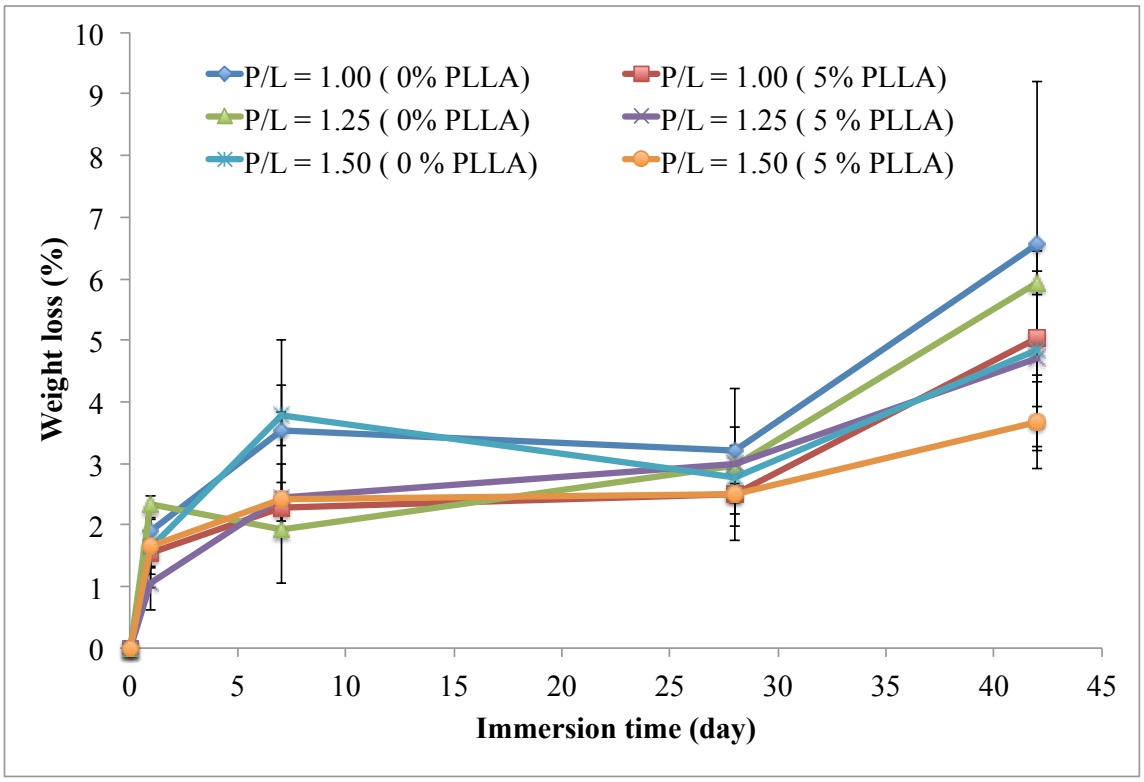

Figure 5.1 Weight loss of the DCPD and PLLA/DCPD composite samples (no sodium citrate additive) during in vitro static degradation.

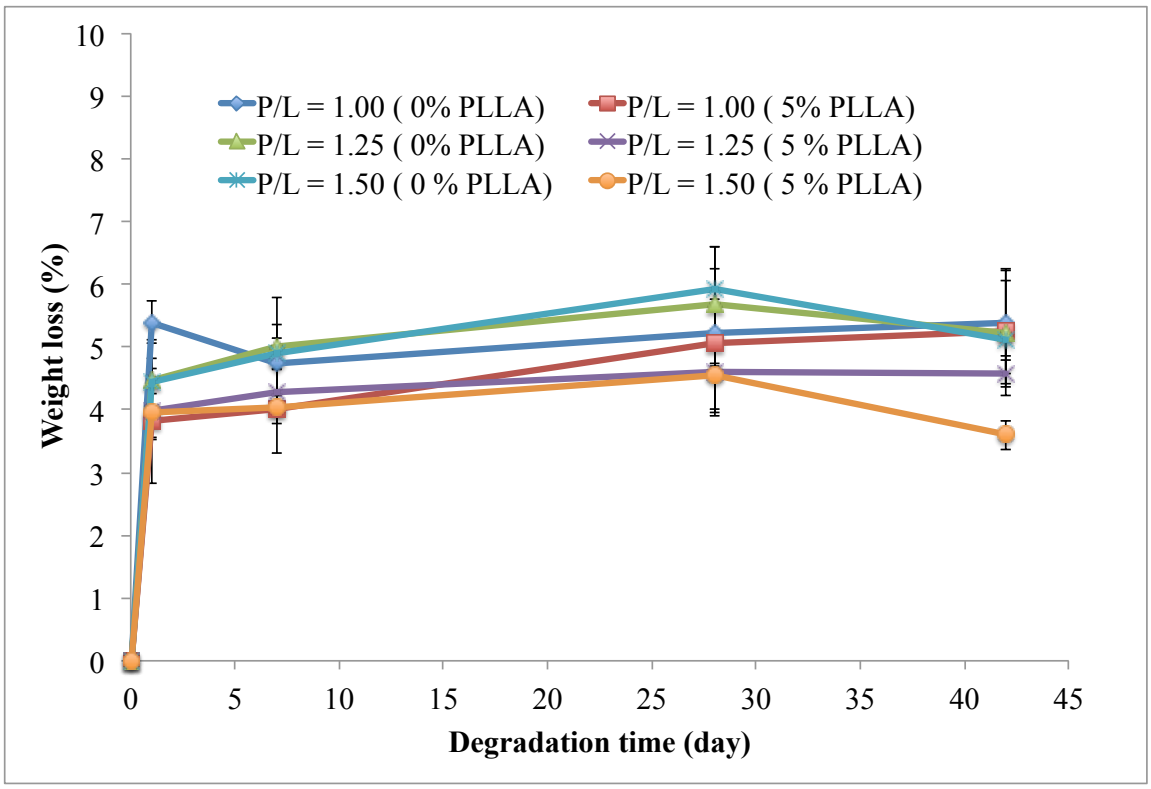

Figure 5.2 Weight loss of the DCPD and PLLA/DCPD composite samples (with sodium citrate additive) during in vitro static degradation.

The variation of pH of PBS solution as a function of immersiton time of DCPD and PLLA/DCPD samples (no sodium citrate additive) was presented in Fig. 5.3. pH value of the PBS sharply decreased after immersion for 1 day. In addtion, the pH of the P/L 1.00 (0% PLLA), P/L 1.00 (5% PLLA), P/L 1.25 (0% PLLA), P/L 1.25 (5% PLLA), P/L 1.50 (0% PLLA), and P/L 1.50 (5% PLLA) groups dropped to 7.4 to 6.93 $\pm$ 0.09, 6.92$\pm$ 0.17, 6.81 $\pm$ 0.24, 7.07$\pm$ 0.17, 6.75 $\pm$ 0.43, and 6.96$\pm$ 0.17, respectively. After that, the pH of the samples gradually decreased and tended to stabilze during day 7 to day 28. After day 28, the pH of the P/L 1.00 (0% PLLA), P/L 1.00 (5% PLLA), P/L 1.25 (0% PLLA), P/L 1.25 (5% PLLA), P/L 1.50 (0% PLLA), and P/L 1.50 (5% PLLA) were sharply reduced to 6.29 $\pm$ 0.12, 6.30$\pm$ 0.10, 6.35 $\pm$ 0.23, 6.11$\pm$ 0.42, 6.25 $\pm$ 0.29, and 6.23$\pm$ 0.09, respectively. The pH follwed the trend of the percentage of weight loss in Fig. 5.1. The pH values sharply dropped after immersion for 7 days due to the

disintergradtion, dissolution and high percent of weight loss of the samples. Then, the pH tended to stablized and followed the trend of weight loss due to the saturation of the solution. After that, the pH values were sharply decreased again due to the further degradation of DCPD as mentioned before. The pH value between 0% PLLA and 5% PLLA groups at each P/L ratio were not significant different at each time point ($p > 0.05$). However, the difference of pH value between 0% PLLA and 5% PLLA tended to be hightest at P/L = 1.50.

The variation of pH of the PBS solutions as a function of immersiton time of DCPD and PLLA/DCPD samples (with sodium citrate additive is presented Fig. 5.4. pH value sharply decreased after immersion for 1 day. In addtion, the pH solution of the P/L 1.00 (0% PLLA), P/L 1.00 (5% PLLA), P/L 1.25 (0% PLLA), P/L 1.25 (5% PLLA), P/L 1.50 (0% PLLA), and P/L 1.50 (5% PLLA) groups were dropped from 7.4 to 6.59 ± 0.05, 6.60 ± 0.05, 6.60 ± 0.03, 6.61 ± 0.02, 6.61 ± 0.04, and 6.57 ± 0.04, respectively. Then, the pH of all the samples tended to stabilize until day 28. After that, the pH of P/L 1.00 (0% PLLA), P/L 1.00 (5% PLLA), P/L 1.25 (0% PLLA), P/L 1.25 (5% PLLA), P/L 1.50 (0% PLLA), and P/L 1.50 (5% PLLA) groups gradually decreased to 6.23 ± 0.20, 6.43 ± 0.01, 6.10 ± 0.25, 6.08 ± 0.22, 6.07 ± 0.26, and 6.05 ± 0.23, respectively. The pH values were sharply dropped after immersion for 1 day due to high percentage of weight loss as mentioned in Fig. 5.2. Then, the pH tended to stablize followed the trend of weight loss due to the saturated solution. After day 28, the pH value decreased a lot while the weight loss did not change much due to the high variation of pH values. In addition, during the experiment, 3 ml of PBS solution was put in the glass vial to put in the incubator as a control group. The result showed that the pH of control group did not significantly changed and was maintained at 7.4 during two week.

The pH results again demonstrated a stronger effect of citrate additive to have a stronger effect on the pH values during degradation, compared to PLLA coating.

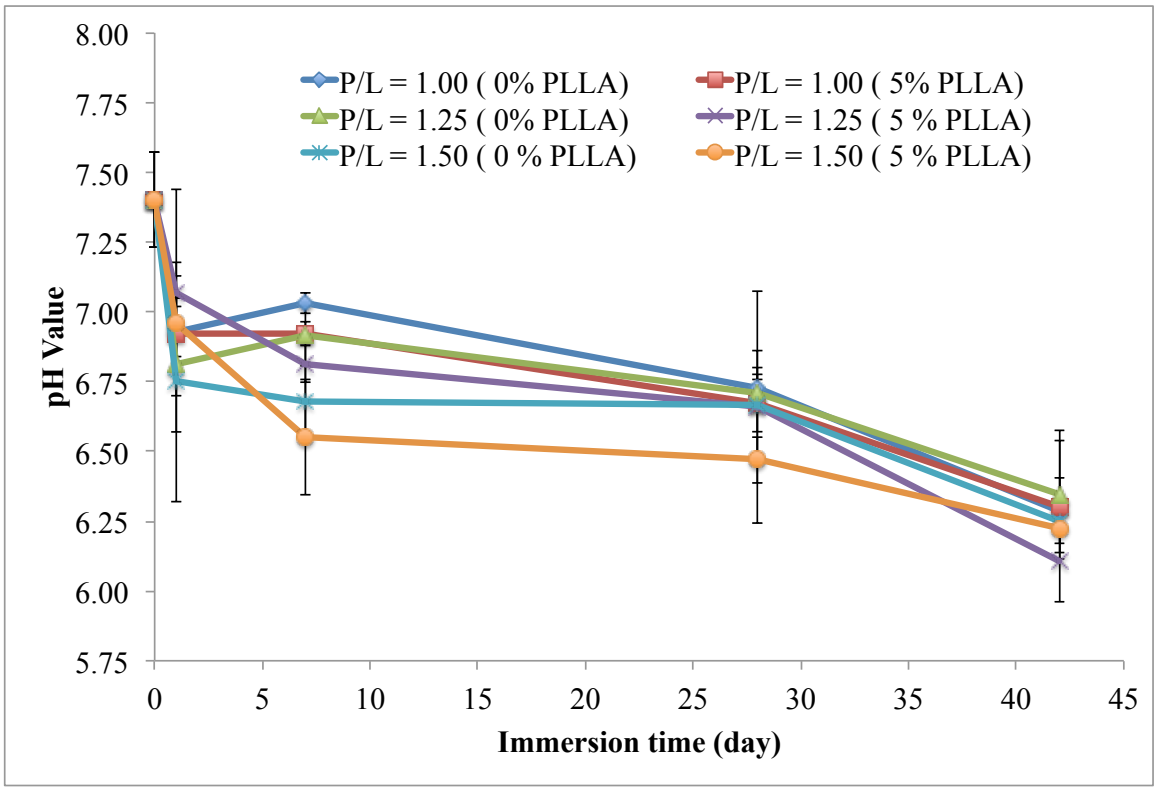

Figure 5.3 pH change of the DCPD and PLLA/DCPD composite samples (no sodium citrate additive) during in vitro static degradation.

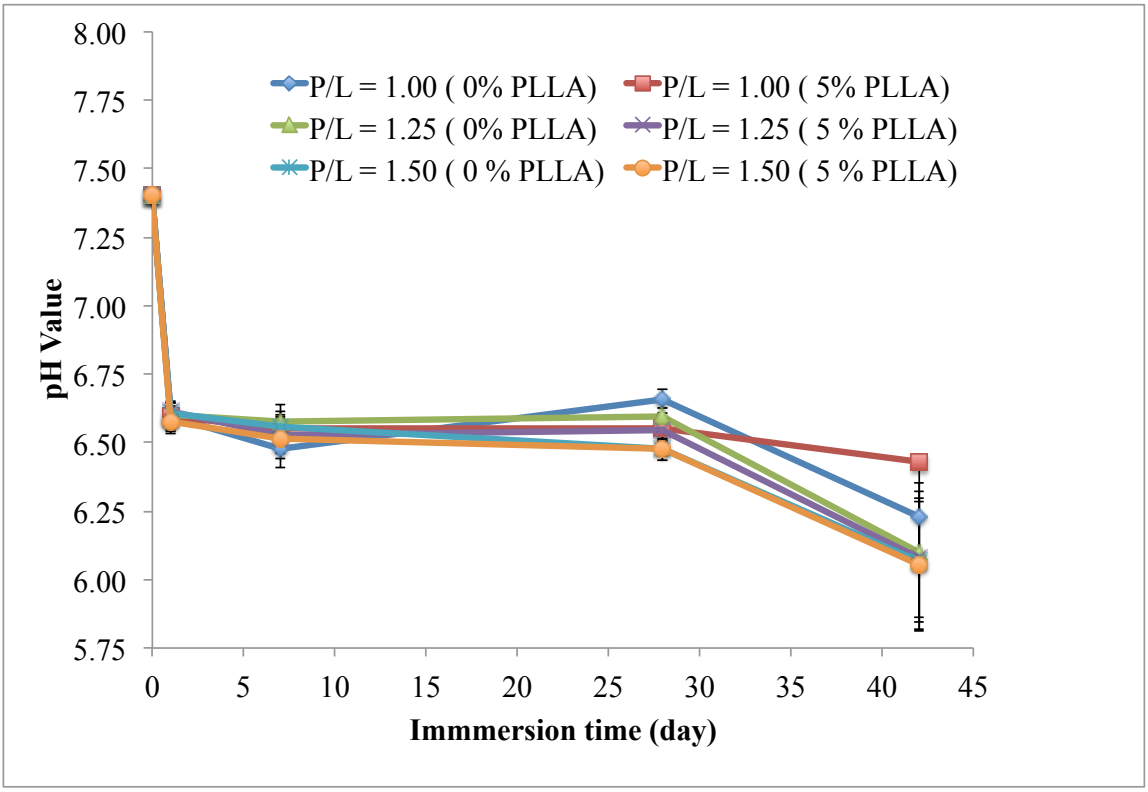

Figure 5.4 pH change of the DCPD and PLLA/DCPD composite samples (with sodium citrate additive) during in vitro static degradation.

The fracture energy versus the degradation time curve of DCPD and PLLA/DCPD composite samples (no sodium citrate additive) were illustrated in the Fig. 5.5. After 7 days of immersion, the fracture energy of the P/L 1.00 (0% PLLA), P/L 1.00 (5% PLLA), P/L 1.25 (0% PLLA), P/L 1.25 (5% PLLA), P/L 1.50 (0% PLLA), and P/L 1.50 (5% PLLA) groups gradually decreased to 0.73 ± 0.03, 1.63 ± 0.23, 1.06 ± 0.36, 2.11 ± 0.48, 1.95 ± 0.24, 2.97 ± 0.55 N-mm, respectively. Then, the curve of the fracture energy tended to stablize until day 28. However, the fracture energy of the P/L 1.25 (5% PLLA) and 1.50 (5% PLLA) were slightly increased due to the high variation of the samples. After that the fracture energy of P/L 1.00 (0% PLLA), P/L 1.00 (5% PLLA), P/L 1.25 (0% PLLA), P/L 1.25 (5% PLLA), P/L 1.50 (0% PLLA), and P/L 1.50 (5% PLLA) were gradully decreased to 1.05 ± 0.31, 1.82 ± 0.55, 1.94 ± 0.70, 3.95 ± 1.15, 1.61 ± 0.62, 4.20 ± 1.24 N-mm, respectively. It was notable that the fracture

energy curves followed the trend of the percent weight loss in Fig. 5.1. After 7 days of immersion, the fracture energy curves were gradually decresed due to high percentage of weight loss of the samples. Then, the curves were stabilized as the percent weight loss were gradually increased and stablized during day 7 to day 28. After that, the fracture energy curves tended to increase according to the mass loss of the samples as mentioned in Fig. 5.1. The fracture energy of the PLLA/DCPD composite samples were not significant higher than the DCPD samples at all P/L ratios except for the initial samples before degradation. However, the largest differences of the fracture energy were found between the PLLA/DCPD composite samples and DCPD samples at P/L 1.50.

The fracture energy versus the degradation time curve of DCPD and PLLA/DCPD composite samples (with sodium citrate additive) were illustrated in the Fig. 5.6. After 7 day of immersion, the fracture energy of the P/L 1.00 (0% PLLA), P/L 1.00 (5% PLLA), P/L 1.25 (0% PLLA), P/L 1.25 (5% PLLA), P/L 1.50 (0% PLLA), and P/L 1.50 (5% PLLA) groups were decreased to 3.00 ± 1.02, 3.62 ± 1.11, 4.28 ± 2.20, 6.55 ± 2.18, 5.14 ± 2.61, 7.09 ± 3.18 N-mm, respectively. The reduction of the fracture energy was due to the high percent weight loss as mentioned from the dissolution and disintegration of the cements. After that, the fracture energy of the samples tended to stabilized follwing the percent weight loss in the Fig. 5.2 due to the saturation of the PBS solution. However, 2 groups of the samples (P/L1.00 (5% PLLA) and P/L 1.25 (5% PLLA)) did not follow the stabilized trend due to the high variation. The fracture energy of P/L 1.00 (5% PLLA) was increased to 5.72 ± 1.58 N-mm while the fracture energy of P/L 1.25 (5% PLLA) was further decreased to 3.90 ± 0.78 N-mm. After day 28, the fracture energy of the samples still stabilized following the trend of the percent weight loss curve. However, the fracture energy of P/L 1.25 (0%) and P/L 1.50 (5%) were increased due to the slightly increased of mass lost with regard to the Fig. 5.2.

The results show that in static degradation, sodium citrate addition has a stronger effect than PLLA coating in that the citrate addition leads to a faster degradation, faster

pH drop, but higher fracture energy in the samples, compared to samples without citrate addition.

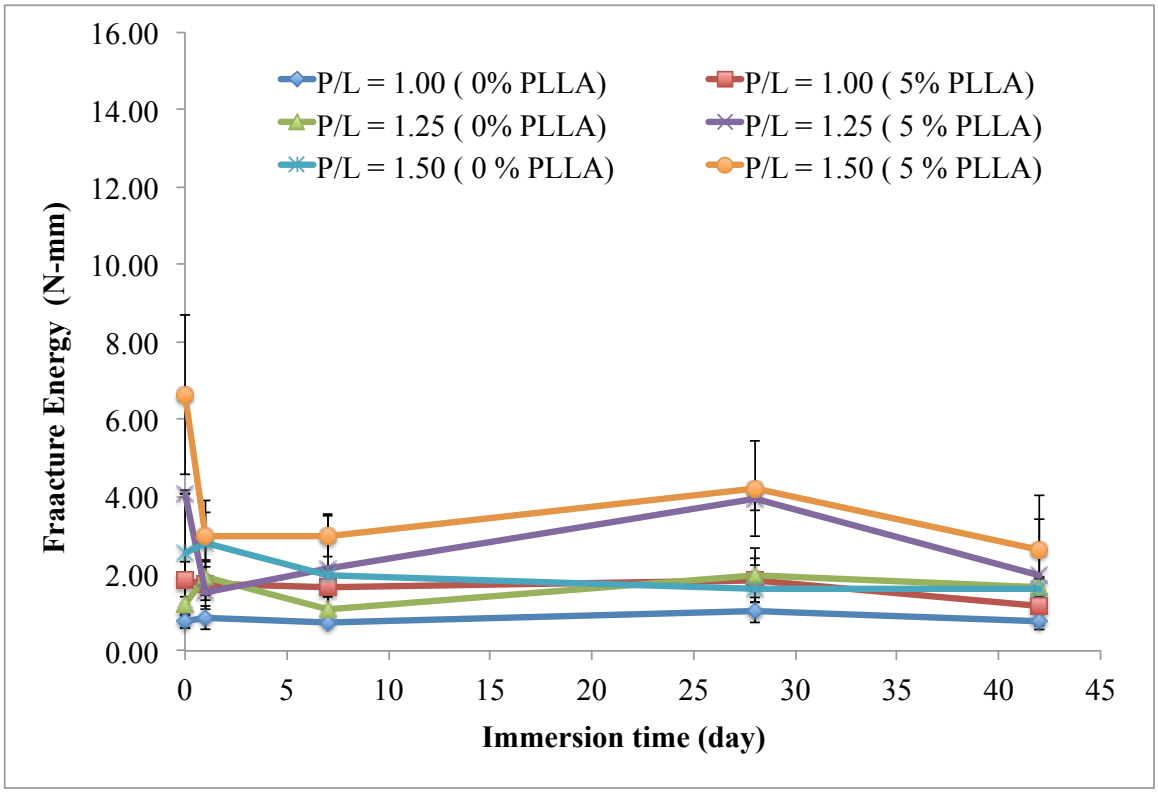

Figure 5.5 Fracture energy versus immersion time curve of the DCPD and PLLA/DCPD composite samples (no sodium citrate additive).

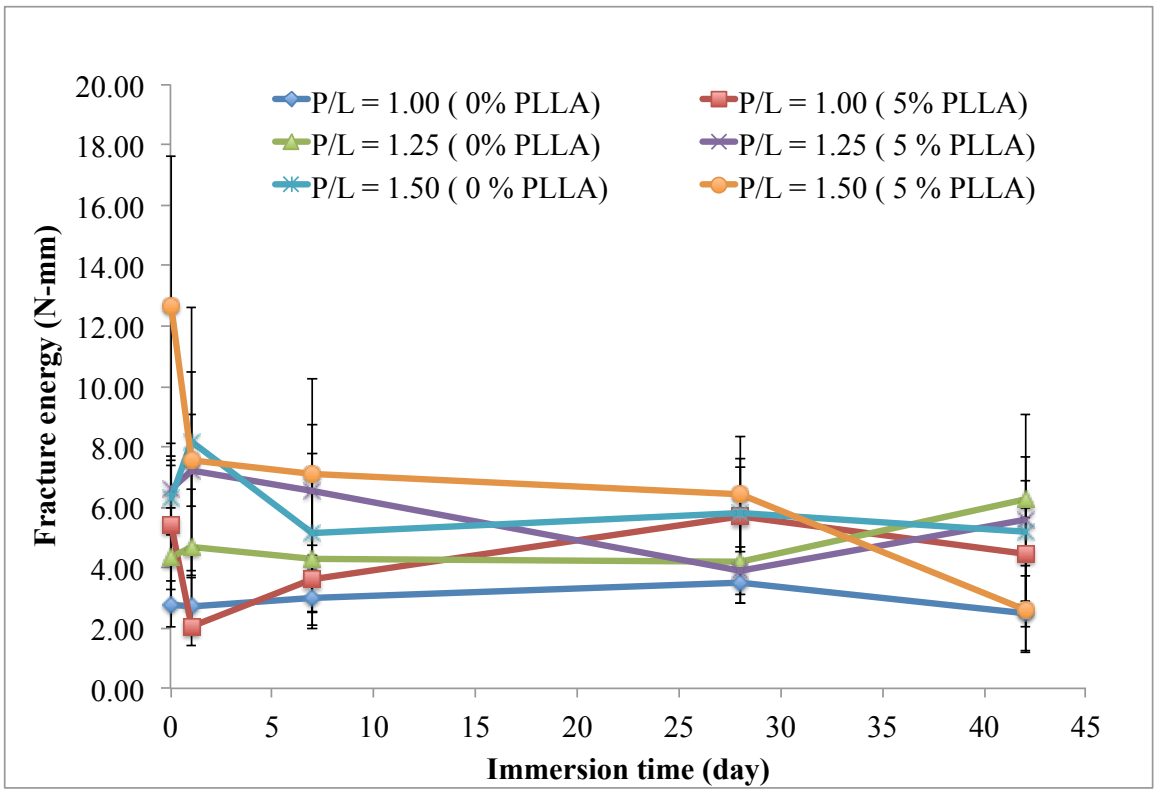

Figure 5.6 Fracture energy versus immersion time curve of the DCPD and PLLA/DCPD composite samples (with sodium citrate additive).

5.4.2 In Vitro Dynamic Degradation

In this experiment, four groups of samples (P/L 1.50 (deionized water, 0% PLLA), P/L 1.50 (deionized water, 5% PLLA), P/L 1.50 (sodium citrate, 0% PLLA), and P/L 1.50 (sodium citrated, 5% PLLA)) were immersed in the PBS solution to study the dynamic degradation behavior up to 56 days and the media was refreshed every 2 weeks.

The percentage of weight loss of the DCPD and PLLA/DCPD composite samples as a function of immersion time was illustrated in the Fig. 5.7. After immmersion in PBS solution for 1 day, the percent weight loss of the P/L 1.50 (deionized water, 0% PLLA), P/L 1.50 (deionized water, 5% PLLA), P/L 1.50 (sodium citrate, 0% PLLA), and (sodium citrate, 5% PLLA) sharply decreased to 1.95 ± 0.33 %, 1.96 ± 0.23 %, 5.30 ± 1.00 %, and 5.11 ± 0.55 %, respectively due to the dissolution and the disintergration of DCPD

cements. After that the percentage of weight loss of the samples tended to stabilize due to the solubility of DCPD reached the limit so that the PBS solution became saturated. After the PBS solution was refreshed on day 14, the percentage of weight loss of the samples gradually increased with time. After immersed P/L 1.50 (deionized water, 0% PLLA), P/L 1.50 (deionized water, 5% PLLA), P/L 1.50 (sodium citrate, 0% PLLA), and P/L 1.50 (sodium citrated, 5% PLLA) groups in PBS solution for 56 day, the percentage of weight loss of these samples were 6.32 % $\pm$ 0.88 %, 7.12 $\pm$ 0.64 %, 7.83 $\pm$ 0.25 %, and 7.29 $\pm$ 0.60 %, respectively. Moreover, the percentage of weight loss between the DCPD and PLLA/DCPD samples using sodium citrate as a liquid component were significantly higher than the samples using deionized water as a liquid component when compared all time points between day 1and day 42 ($p < 0.05$). However, the weight loss of DCPD samples and PLLA/DCPD composite samples were not significantly different during in vitro dynamic degradation ($p > 0.05$).

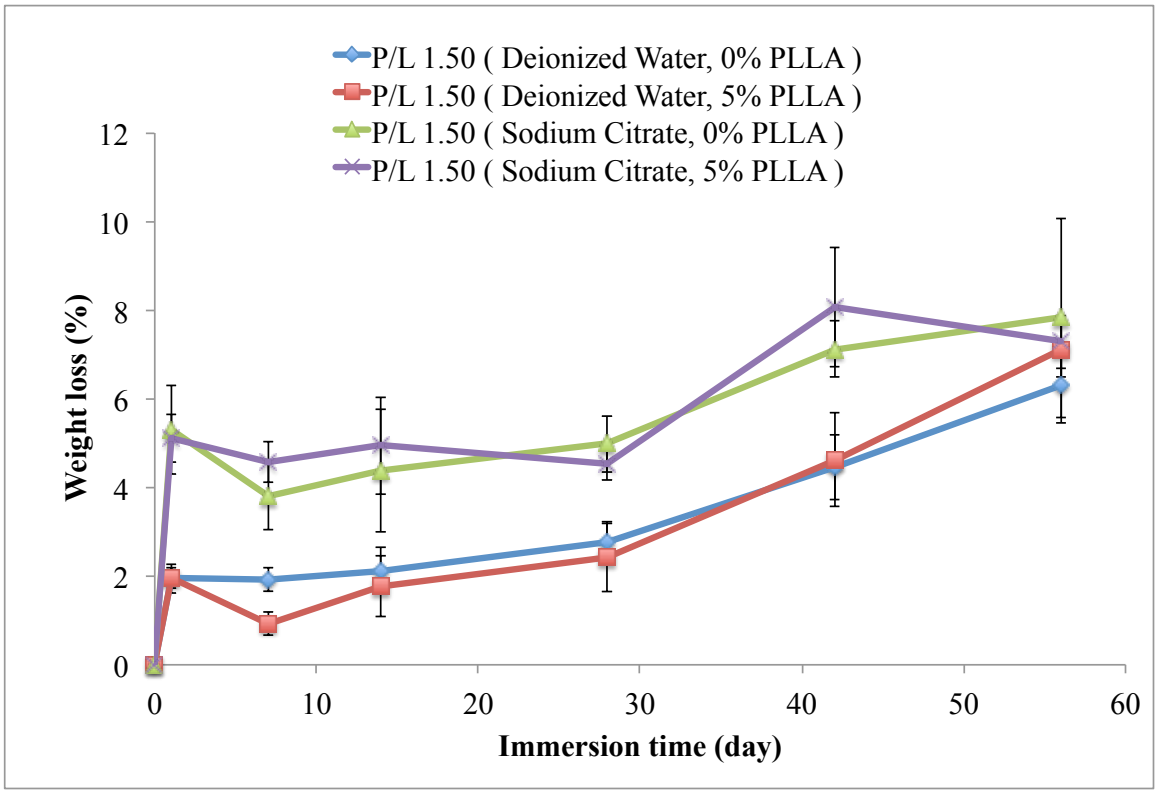

Figure 5.7 Weight loss of the DCPD and PLLA/DCPD composite samples as a function of immersion time during in vitro dynamic degradation.

The pH variation of PBS solution as a function of immersion time is illustrated in Fig. 5.8. The pH values of the four groups sharply decreased after immersion in PBS for 1 day due to the high intial weight loss of the samples. Then, the pH values gradually decreased and stabilized during day 1 to day 14 corresponed to the percent weight loss curve in the Fig. 5.7. After day 14, the pH values of the samples gradually increased. After being immersed for 42 days, the pH of P/L 1.50 (deionized water, 0% PLLA), P/L 1.50 (deionized water, 5% PLLA), P/L 1.50 (sodium citrate, 0% PLLA), and P/L 1.50 (sodium citrated, 5% PLLA) groups reached to 6.86 ± 0.10, 6.87 ± 0.10, 6.98 ± 0.10, and 6.98 ± 0.10, respectively. After that , the pH values of P/L 1.50 (deionized water, 5% PLLA), P/L 1.50 (sodium citrate, 0% PLLA), and P/L 1.50 (sodium citrated, 5% PLLA) groups decreased to 6.72 ± 0.09, 6.74 ± 0.31, and 6.85 ± 0.07, respectively. However, the pH value of P/L 1.50 (deionized water, 0% PLLA) group did not change.

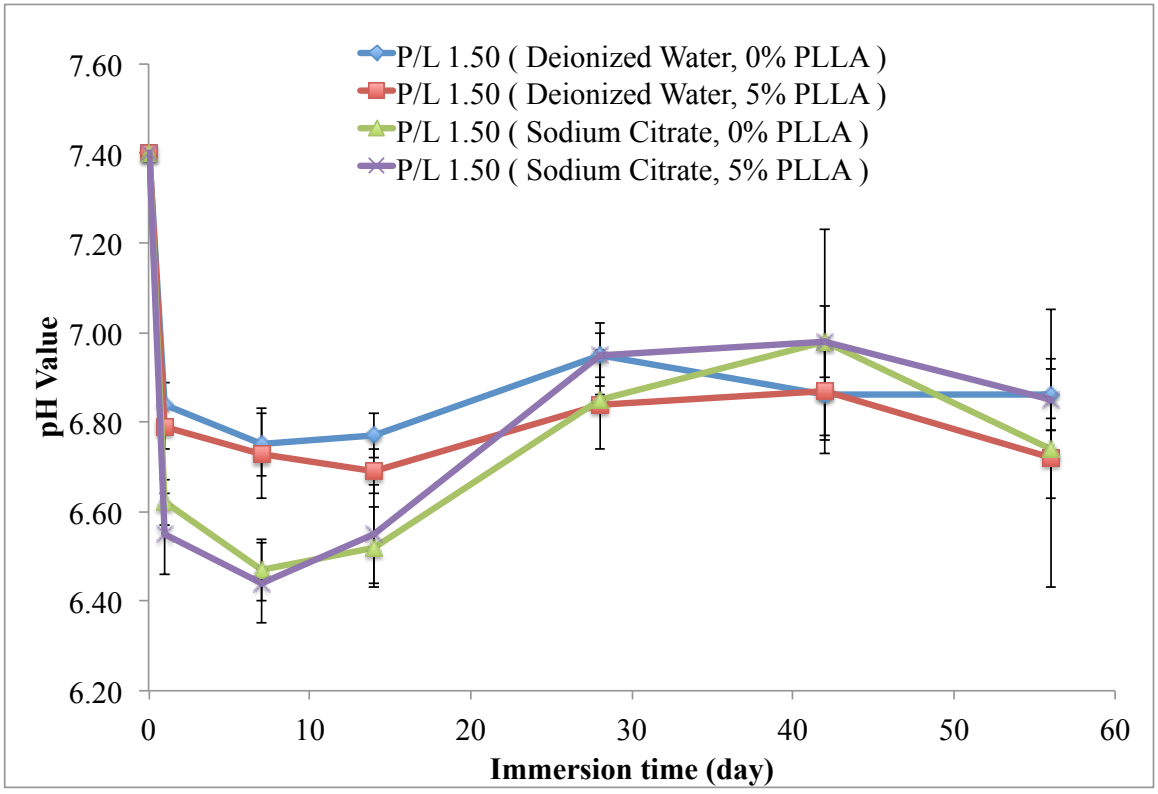

Figure 5.8 Variation of pH values of the DCPD and PLLA/DCPD composite samples as a function of immersion time during in vitro dynamic degradation.

The fracture energy versus the degradation time curve of DCPD and PLLA/DCPD composite samples were illustrated in Fig. 5.9. The overall fracture energy of all the groups except P/L 1.50 (deionized water, 0% PLLA) decreased after immersion for 56 days. The fracture energy of the P/L 1.50 (deionized water, 0% PLLA) did not decreased when compared to day 0 due to the high variation of the initial samples. The reason of the decreasing of fracture energy after immersion were probably due to the dissolution of calcium phosphate cement phase, which contained soluble salts, [45] and transformation of calcium phosphate cements [46, 47]. The conversion of dicalcium phosphate dihydrate (DCPD) to dicalcium phosphate anhydrous (DCP) was found to be detrimental for the strength of the cements resulted in the decrease of the fracture energy of the samples after immersion [46, 47].

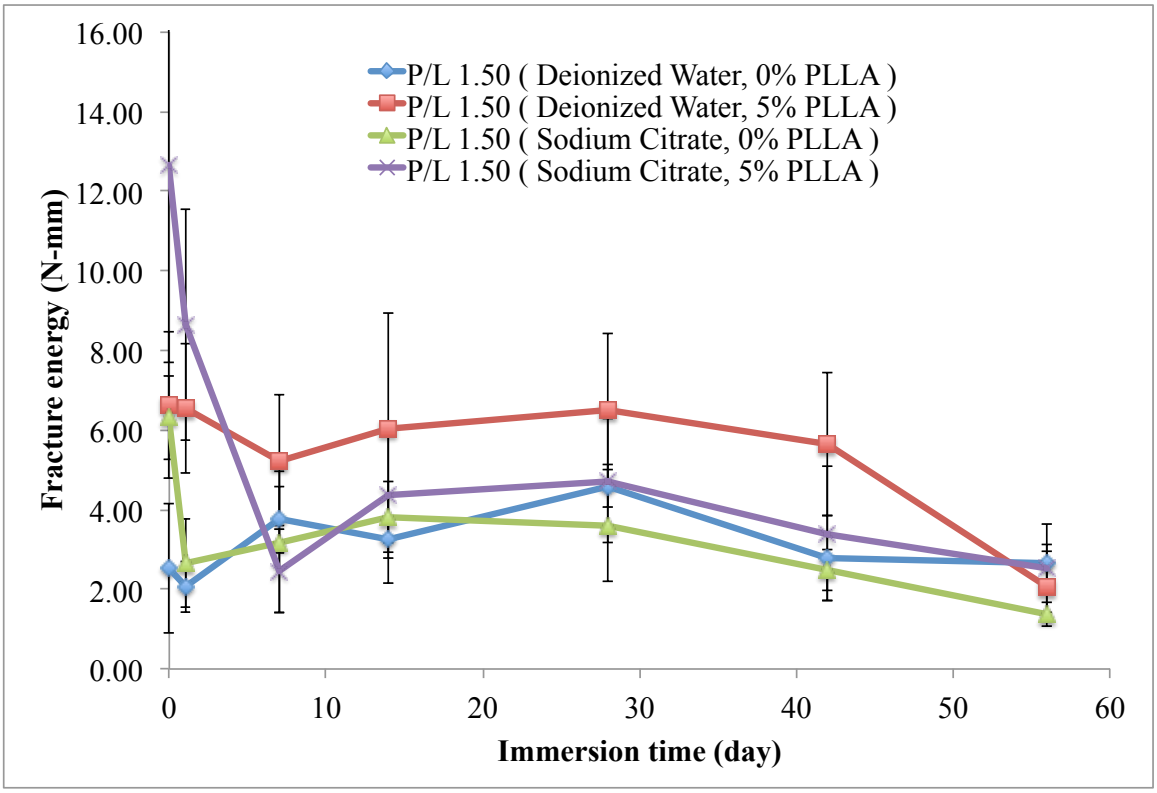

Figure 5.9 Fracture energy of the DCPD and PLLA/DCPD composite samples as a function of immersion time during in vitro dynamic degradation.

In vitro degradation behavior of DCPD and PLLA/DCPD composite samples in PBS solution were investigated through characterizing the variation of the percentage of weight loss, the pH value and the fracture energy. The percentage of weight loss of the samples increased as time. The changes of the pH values corresponded to the percentage of weight loss of the samples. Transformation of brusihte cements to hydroxyapatite (HA) was caused by 3 mechanisims: dissolution, disintegration, and conversion [31]. The difference of the percentage of weight loss between dynamic and static degradations ocurred due to the saturation of the ageing medium (PBS solution) with regarded to calcium ions [33]. Since the PBS solution had no calcium ions, once the samples were placed, the DCPD dissolution could begin to increase the amount of calcium and phosphate ions in the solution. As a result, the slowing rate of the degradation was detected according to higher concentration of calcium and phosphate ions in the solution. When the dissolution products were removed every two weeks by refreshing the PBS solution, the basis of higher dissolution rate was maintained. In addition, higher dissolution also lead to the disintegration of DCPD. The formation of HA might ocurr due to the persistent removal of the ions in the solution allowing the DCPD to dissolve and reprecipitate as HA. The decrease of pH after day 28 occurred might because of the phosphoric acid, which was a by-product from the conversion of DCPD to HA as mentioned in the following equation.

$$10CaHPO_4 \cdot 2H_2O \rightarrow Ca_{10}(PO_4)_6(OH)_2 + 4H_3PO_4 + 18H_2O \qquad (2.6)$$

The surfaces of the P/L 1.50 (deionized water, 0% PLLA), P/L 1.50 (deionized water, 5% PLLA), P/L 1.50 (sodium citrate, 0% PLLA), and P/L 1.50 (sodium citrated, 5% PLLA) groups during in vitro dynamic degradation were investigated by a scanning electron microscope (SEM, JEOL JSM-5310LV) up to 56 days.

The PLLA coating can be clearly seen in Fig. 5.11. Small needle-like precipitation can be seen on the surface of the coating on day 7. The precipitation becomes very apparent at day 56. The precipitation is presumed to be HA. The actual

crystalline nature of the precipitate will be analyzed in the future. Fig. 5.12 shows the effect of sodium citrate in inducing a finer crystalline structure in DCPD. The finer crystalline structure is presumed to allow a more even PLLA coating seen in Fig. 5.13. The PLLA coating can be seen to show porosity starting from day 7. At the same time, the needle shape precipitation as seen in the distilled water group are also seen here in the sodium citrate samples.

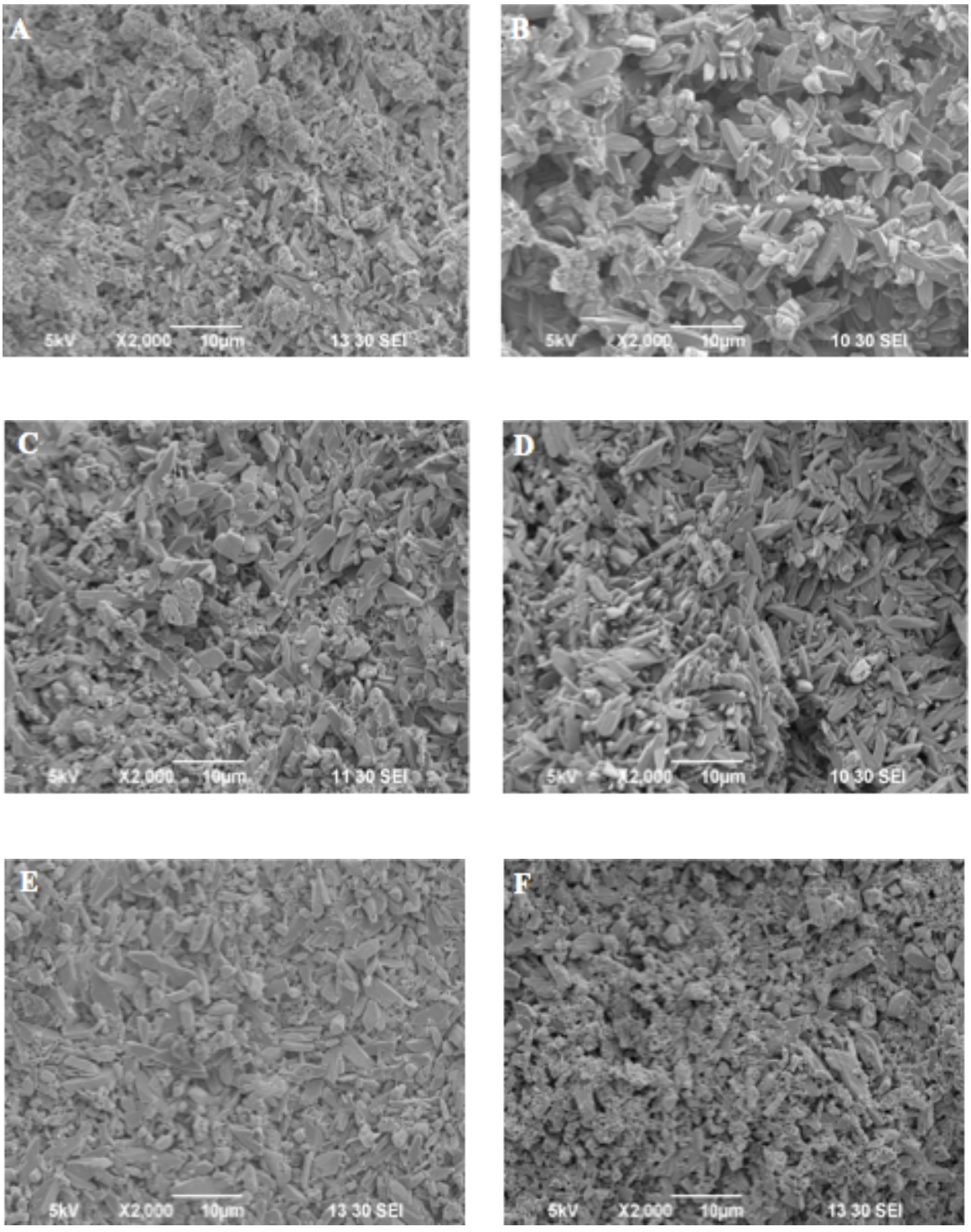

Figure 5.10 SEM images of the surface of the DCPD samples (Deionized Water, 0% PLLA) after immersion in PBS for 1 day (A), 7 days (B), 14 days (C), 28 days (D), 42 days (E), and 56 days (F).

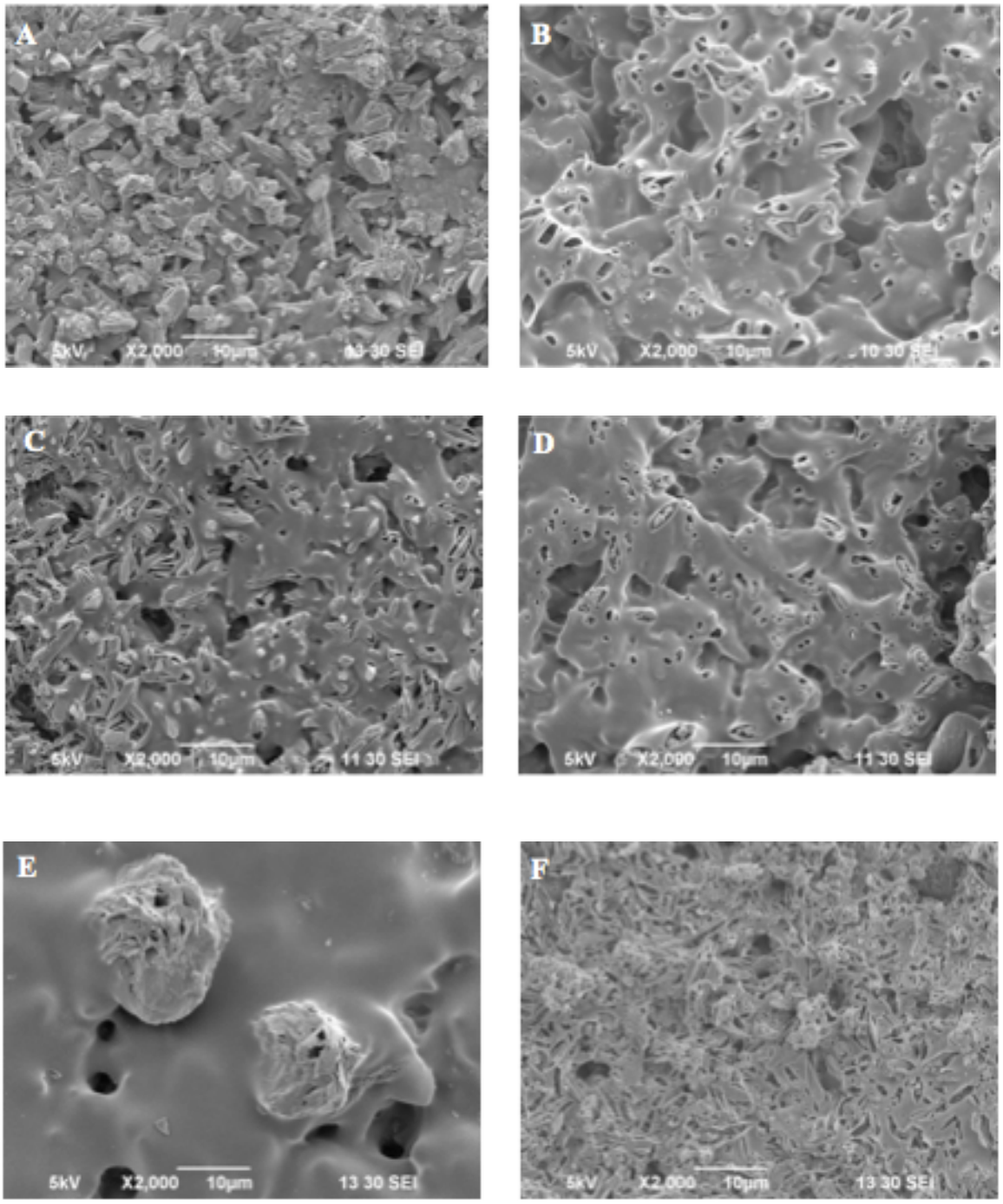

Figure 5.11 SEM images of the surface of the DCPD samples (Deionized Water, 5% PLLA) after immersion in PBS for 1 day (A), 7 days (B), 14 days (C), 28 days (D), 42 days (E), and 56 days (F).

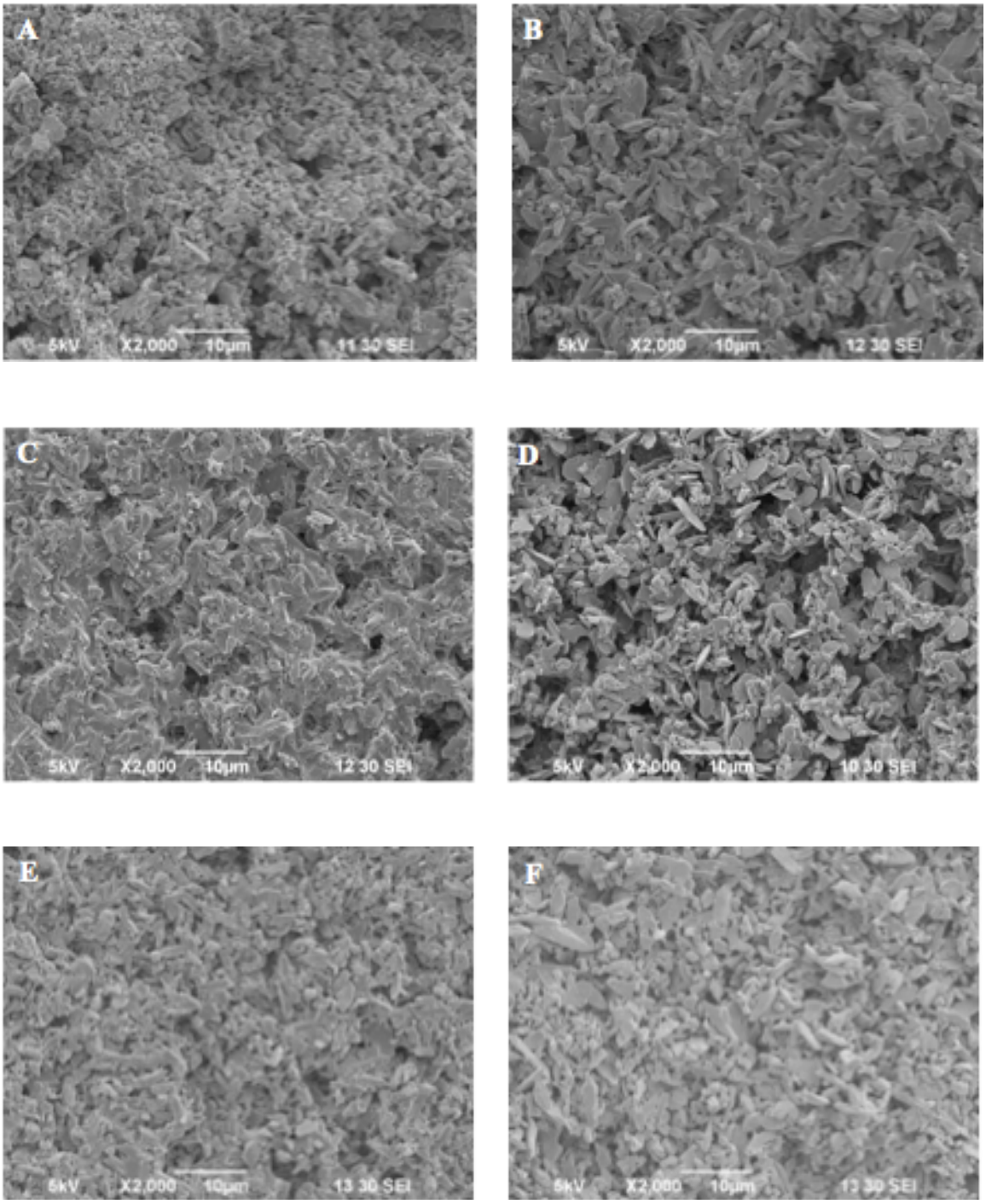

Figure 5.12 SEM images of the surface of the DCPD samples (Sodium Citrate, 0% PLLA) after immersion in PBS for 1 day (A), 7 days (B), 14 days (C), 28 days (D), 42 days (E), and 56 days (F).

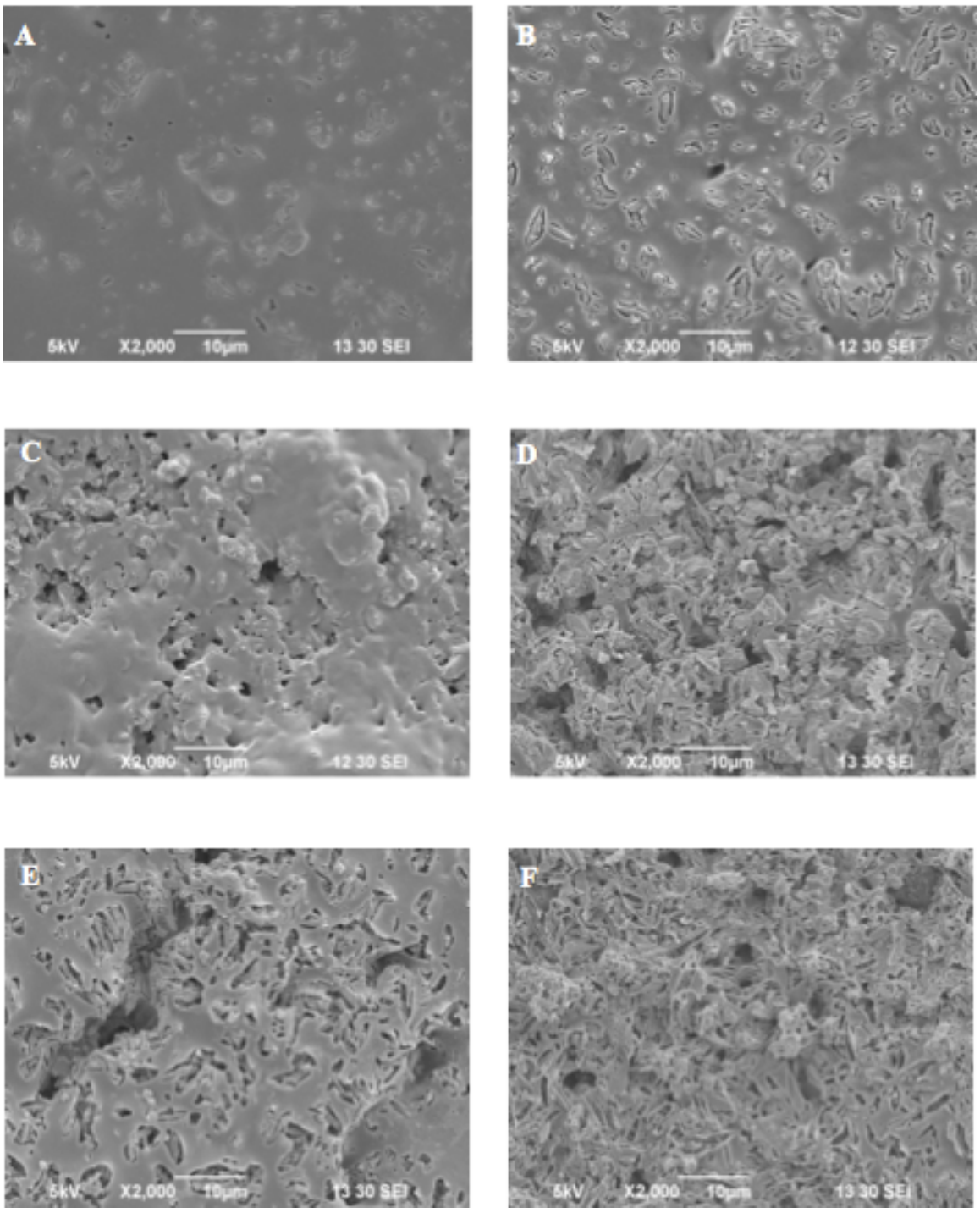

Figure 5.13 SEM images of the surface of the DCPD samples (Sodium Citrate, 5% PLLA) after immersion in PBS for 1 day (A), 7 days (B), 14 days (C), 28 days (D), 42 days (E), and 56 days (F).

6. IN VITRO BIOCOMPATIBILITY ANALYSIS

6.1 Introduction

Brushite has been proved biocompatible and osteoconductive in vivo however only a few studies were documented under in vitro condition [8, 13]. In this study, DCPD samples with and without PLLA coating were fabricated to investigate the cytocompatibility under in vitro condition. In addition, the viability, differentiation, and the morphologies of dog bone marrow stromal stem cells (dBMSCs) on the surface of the samples were investigated.

6.2 Sample Preparation

Two groups of samples were prepared using MCPM (Strem Chemicals, New Buryport, MA) and β-TCP (Fluka Chemical corperation, Ronkonkoma, NY) with the ratio of MCPM to β-TCP = 1:1 and P/L = 1.50. Two different types of solutions were used to prepare two major groups of samples. The first major group was fabricated using deionized water as a liquid component. The other major group was prepared by using a 100 mM sodium citrate solution (Fisher Scientific, Pittsburgh, PA) as the liquid component.

Two powder components (MCPM and β-TCP) were measured corresponding to the molar ratios mentioned above by a balance (Mettler AE 100). The two powders were hand mixed in a mortar to ensure homogeneity. Then, the powders and liquid components were mixed at P/L = 1.50 by a metal spatula to ensure a homogenous slurry. After that, the slurry was casted into an aluminum mold to form disk samples (5 mm diameter and 2.5 mm thickness). After allowing the cement paste to set for 8 min, the samples were

removed from the mold. Then, the samples were dried in a vacuum desiccator chamber at room temperature for 48 h.

For the composite DCPD/PLLA samples preparation, two groups of DCPD disk samples (no additive and with sodium citrate additive) as mentioned above were fabricated. After that, PLLA pellets were dissolved in chloroform ($CHCl_3$) solvent (5 %). The DCPD disk samples were immersed into PLLA solution under chemical hood. Then, the samples were taken out and dried in vacuum desiccator chamber at room temperature for 48 h. In this experiment, four groups of DCPD disk samples were fabricated corresponding to Table 6.1.

Table 6.1 Four groups of samples for biocompatible testing

Group	Liquid phase	P/L	PLLA
1	Deionized water	1.50	Uncoated PLLA
2		1.50	Coated 5% PLLA
3	Sodium citrate	1.50	Uncoated PLLA
4		1.50	Coated 5% PLLA

6.3. Experimental Procedure

6.3.1 Assessment of Cell Viability

To evaluate the effect of cement on the viability of the dBMSCs, six DCPD disk samples of each group corresponding to Table 6.1 were soaked individually with 2 ml of phosphate buffer solution (PBS) for 7 days. Moreover, the PBS was changed every 24 h. After that, the samples were sterilized by soaking in 70% ethanol for 30 min and washed with PBS for two times. Then, the samples were soaked individually in 550 μl of cell culture medium (Dulbecco's modified eagles medium (Invitrogen, Carlsbad, CA) supplemented with 10% fetal bovine serum (Atlanta Biologicals, Lawrenceville, GA),

and 1% antibiotic-antimycotic solution). After 24 h, the conditioned medium was pipetted out to culture the cells.

The effect of the conditioned medium on cell proliferation was evaluated on dBMSC as previously described [31]. The cells were placed at 2,000 cells/well in a 96-well plate. After the cells had attached for one day, they were cultured in 100 μl conditioned medium that was soaked with a sample for 24 h. The cultured medium was changed every second day from the conditioned medium soaking the samples; soaking medium of the sample was refreshed at the same time. The test was performed on days 1, 3, and 7 with XTT assay. The XTT solution was prepared by mixing 1 mg/ml of XTT sodium salt (2,3-Bis(2-methoxy-4-nitro-5-sulfophenyl)-2*H*-tetrazolium-5-carboxanilide inner salt, Sigma-Aldrich, St.Louis, MO) labeling reagent in DMEM without phenol red with 0.383 mg/ml of PMS (Phenazine methosulfate, Sigma-Aldrich, St.Louis, MO). On each XTT testing day, 50 μl of the XTT solution was added to each well of the cell culture well plate and incubated for 4 h at 37℃. Then, 100 μl of solution in well was taken to test the spectrophotometrical absorbance of the samples at 450 nm using microplate reader (THERMOmax, Molecular Devices) and 650 nm wavelength was used as a reference. In addition, standard non-conditioned DMEM medium was used as a positive control.

6.3.2 Assessment of Alkaline Phosphatase (ALP)

To evaluate the effect of cement on the differentiation of dBMSCs, six DCPD disk samples of each group corresponding to the Table 6.1 were soaked individually with 2 ml of phosphate buffer solution (PBS) for 7 days. Moreover, the PBS was changed every 24 h. After that, the samples were sterilized by soaking in 70% ethanol for 30 min and washed with PBS for two times. Then, the samples were soaked individually in 550 μl of cell culture medium (Dulbecco's modified eagles medium (Invitrogen, Carlsbad, CA) supplemented with 10% fetal bovine serum (Atlanta Biologicals, Lawrenceville, GA), 1% antibiotic-antimycotic solution) additioned with osteogenic factors (10^{-8} M

dexamethansone, 5 μg/ml ascorbic acid, 2-phosphate, and 20 mM β-glycerophosphate). After 24 h, the conditioned medium was pipetted out to culture the cells.

Then, the effect of the conditioned medium on cell differentiation were evaluated on dBMSCs via ALP activity as previously described [31]. The cells were placed at 5,000 cells/well in a 96-well plate. After the cells had attached and proliferated for three days, they were cultured in 150 μl conditioned osteogenic medium that was soaked with a sample for 24 h. The cultured medium was changed every second day from the conditioned osteogenic medium soaking the samples; soaking medium of the sample was refreshed at the same time.

The ALP activity was performed on day 3, 7, and 14 with alkaline phosphatase (ALP) assay kit (Sigma-Aldrich, St. Louis, MO). Furthermore, the standard non-conditioned osteogenic medium was used as a positive control. At each time point, the cells were washed with PBS. Then, they were lysed in 0.2% Triton X-100 solution and undergone three freeze/thaw cycles (-80/37 $°C$) for 60 min in total. The cell lysates were placed in a 96-well plate to measure the ALP activity with p-nitrophenyl phosphate (p-NPP) substrate as described in the manufacturer's manual. The fluorescence was measured by a fluorometer (SpectraMax, Molecular Devices) at 360 nm excitation and 440 nm emission.

6.3.3 Cell Morphologies

To investigate the cell morphologies and cell attachment on the DCPD disk samples with and without PLLA coating, six DCPD disk samples of each group corresponding to the Table 6.1 were soaked individually with 2 ml of phosphate buffer solution (PBS) for 7 days. Moreover, the PBS was changed every 24 hours. After that, the samples were sterilized by soaking in 70% ethanol for 30 min and washed with PBS for two times. Then, the samples were soaked individually in 550 μl of cell culture medium (Dulbecco's modified eagles medium (Invitrogen, Carlsbad, CA) supplemented with 10%

fetal bovine serum (Atlanta Biologicals, Lawrenceville, GA), and 1% antibiotic-antimycotic solution). After 24 h, the samples were removed and placed into a 96-well plate. After that, each sample was seeded with 2000 dBMSCs and incubated in 100 μl culture medium. At each time point (Day 1 and 7), the samples were transferred into a new 48-well plate and rinsed with PBS (pH 7.4) for two times. Then, they were fixed with 4% formaldehyde. The samples were transferred to a new 24-well plate. Then, the fixed cells were washed with PBS with for 5 min and followed by sequential dehydration in graded ethanol (50%, 70%, 80%, 95%, and 100%, each 10 min). After that, the samples were dried in sequential hexamethyldisilizane (HDMS) solution and sputter coated with gold for SEM analysis. The morphologies of the cells on the surface of samples were observed by a scanning electron microscope (SEM, JEOL JSM-5310LV).

6.3.4 Statistical Analysis

Three-way analysis of variance (ANOVA) with the post hoc Tukey-Kramer multiple-range test was applied to determine significant differences of the XTT and ALP results normalized to the positive controls. A level of $\alpha = 0.05$ was used for statistical significance.

6.4 Results and Discussion

6.4.1 Cell Attachment and Mophologies

Fig. 6.1 showed the dBMSC morphology on DCPD and PLLA/DCPD composite samples after 1 and 7 days of culture. The cells were found to be able to attach and spread on the surface of the DCPD and PLLA/DCPD composite samples after seeding for 1 day. A slight increased number of cells was observed on DCPD samples (no sodium citrate and with sodium citrate additive) when comparing day 7 to day 1. However, the cells, on the surface of PLLA/DCPD groups (no sodium citrate and with sodium citrate additive)

was difficult to observe via SEM images PLLA coating. Therefore the difference of the cell number on the surface of the composites compared between day 1 and day 7 were difficult to observe.

	DCPD (No Sodium Citrate Additive)	**PLLA-Coated DCPD (No Sodium Citrate Additive)**
Day 1	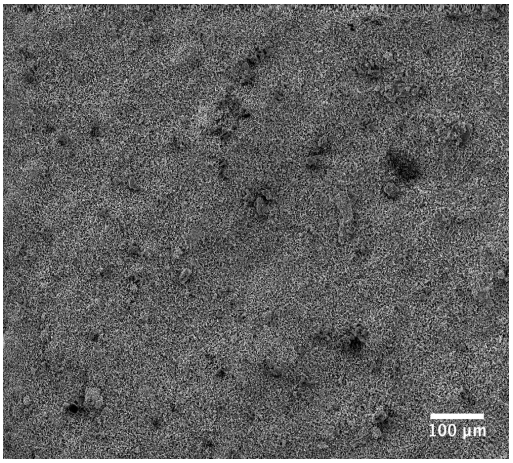	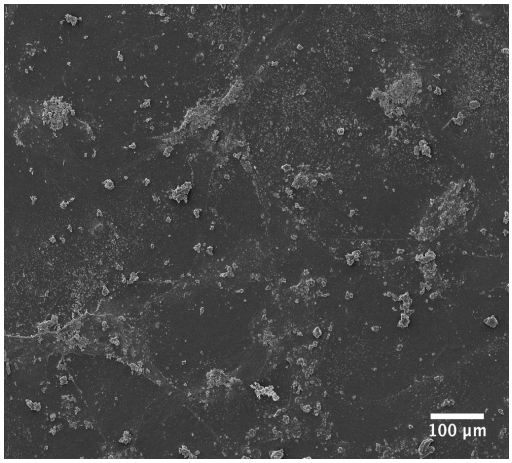
	DCPD (With Sodium Citrate Additive)	**PLLA-Coated DCPD (With Sodium Citrate Additive)**
Day 1	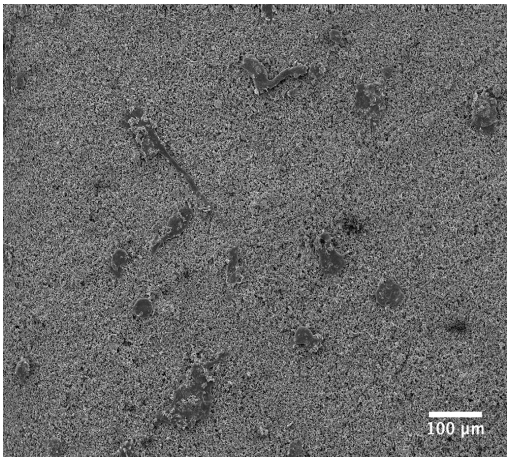	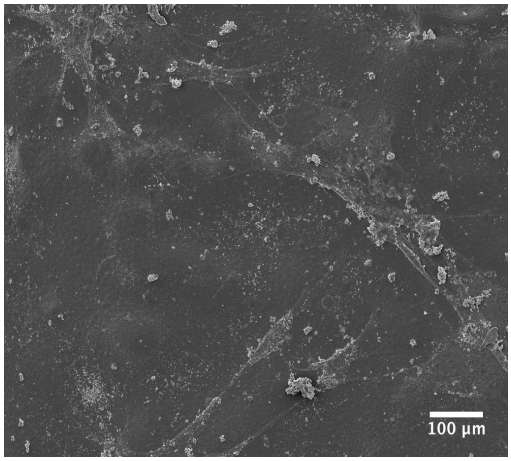

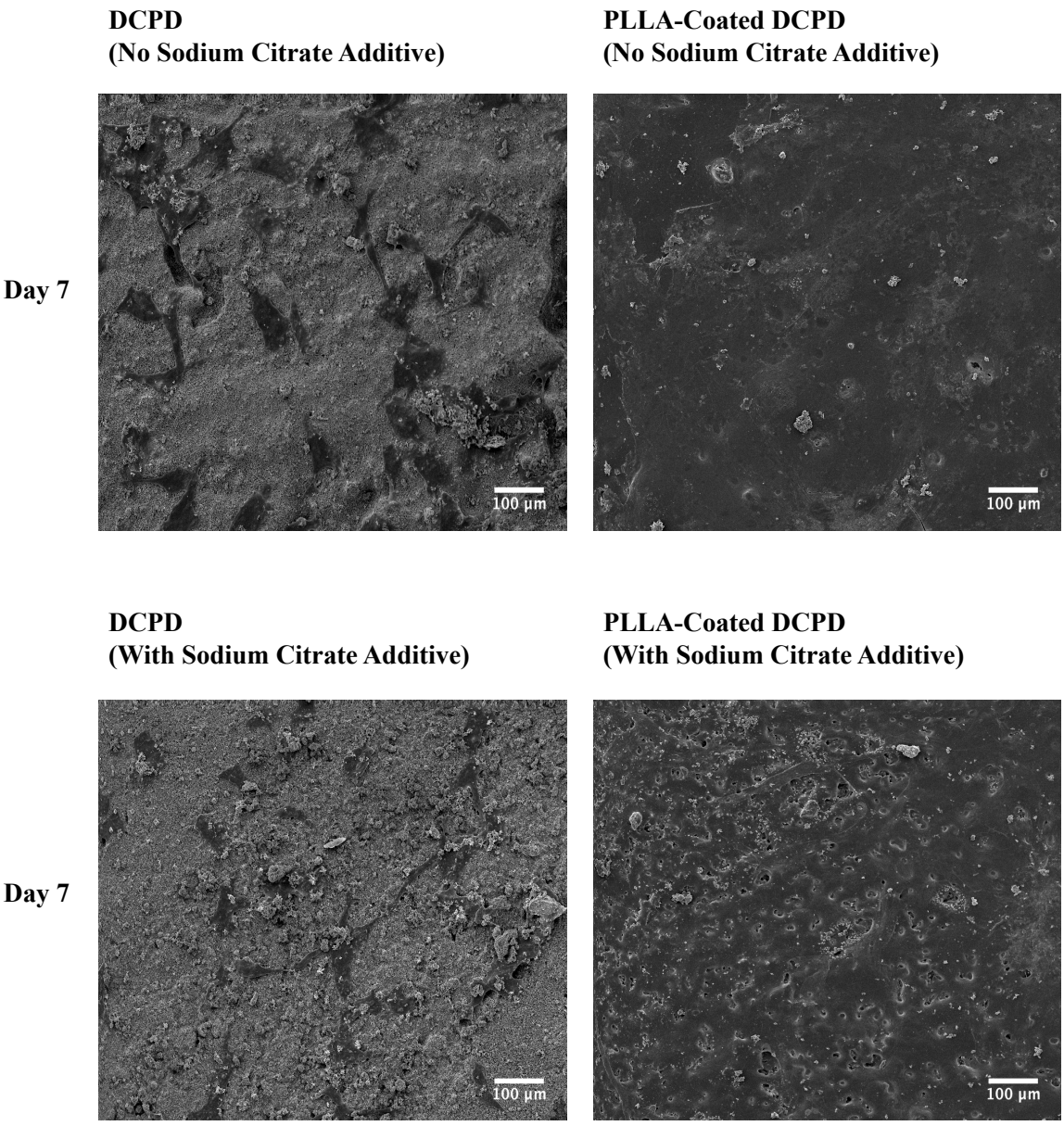

Figure 6.1 SEM images of the morphology of dBMSCs on the DCPD (with and without sodium citrate additive) and PLLA-coated DCPD (with and without sodium citrate additive) at day 1 and 7.

6.4.2 Cell Proliferation

The dBMSCs proliferation was investigated by XTT after cultured in the medium that conditioned with DCPD and PLLA/DCPD composite samples for 1, 3, and 7 days (Fig. 6.2). Fig. 6.2 demonstrated the percentage of cell numbers compared to the positive control (standard DMEM medium). From the three-way ANOVA analysis, the results showed that day 1 was significantly lower than day 3 ($p< 0.05$) and day 7 ($p< 0.05$) but day 3 and day 7 were not significantly different from each other. These results suggested the cells were still viable regardless of the different trends. Two groups of samples ((no additive, 0% PLLA) and (with sodium citrate additive, 5% PLLA)) had shown the cell proliferation trend, which was the percentage to positive control increased with the incubation time. However, another two groups showed no trends with the incubation time.

In addition, the percentage to positive control of 5% PLLA coated DCPD samples was significantly higher than 0% PLLA without sodium citrate ($p < 0.05$) but the effect of PLLA coating was not significantly different with sodium citrate groups ($P > 0.05$). Some studies showed that brushite cements caused rapidly decreased pH in vivo after implantation [11, 48, 49]. The phenomenon might affect the cell viability on the samples. Therefore, coating 5% PLLA on the samples might slow down the pH reduction during culture periods resulting in the high percentage to positive control on PLLA-coated DCPD samples. The percentage to positive of the samples containing sodium citrate was significantly higher than no sodium citrate with 0% PLLA ($p <0.05$) but sodium citrate had no significant effect with 5% PLLA ($p > 0.05$). These results suggested that the DCPD and PLLA/DCPD composite samples were compatible with dBMSCs and the cells were able to proliferate in the conditioned medium.

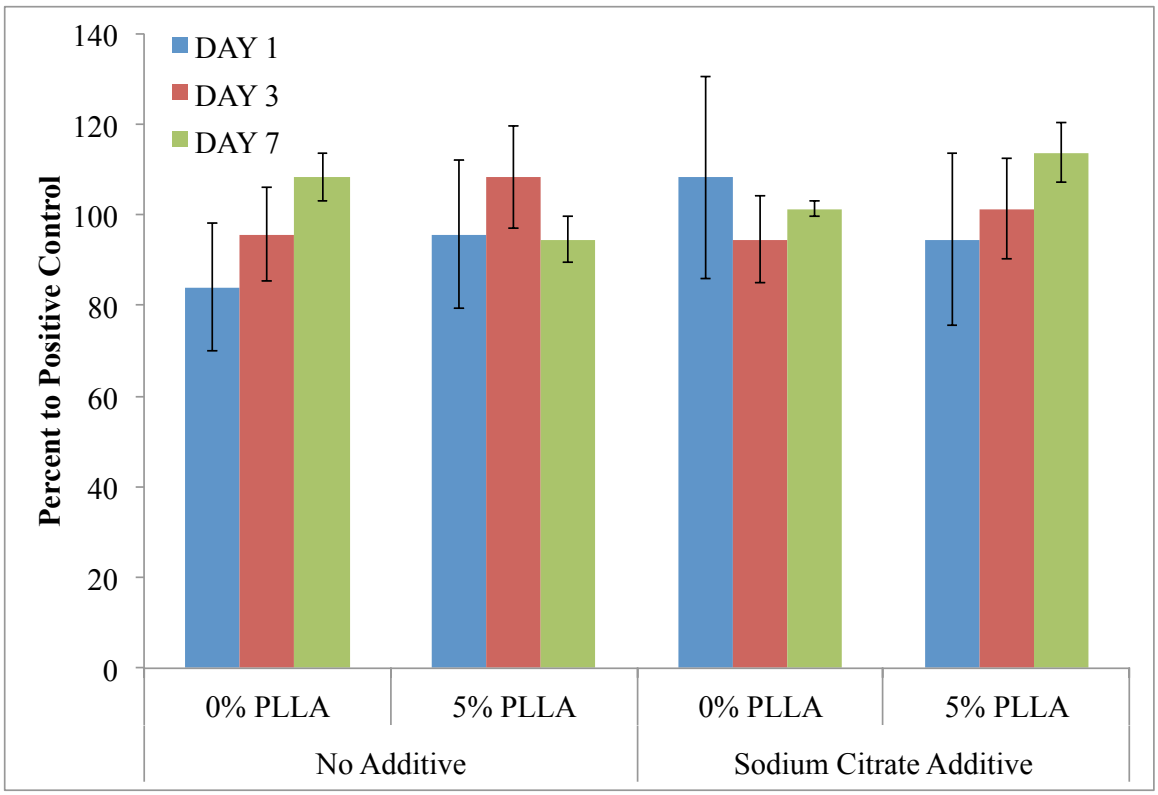

Figure 6.2 The percentage to positive control (XTT) of dog bone marrow stromal stem cells cultured in the medium conditioned with DCPD or PLLA-coated DCPD samples. The standard DMEM medium was used as positive control.

6.4.3 Cell Differentiation

Alkaline phosphatase is the most commonly recognized early biomarker for osteogenic differentiation during the in vitro experiment. Alkaline phosphatase activity of dBMSCs cultured in the medium conditioned with the DCPD and PLLA/DCPD (with and without sodium citrate additive) samples for 3, 7, and 14 days were demonstrated in Fig. 6.3. The figure shows that the ALP enzyme activity of dBMSCs cultured in the conditioned medium slightly increased from day 3 to day 7. From three-way ANOVA, the ALP enzyme activity significantly decreased on day 14 ($p < 0.05$). Some studies reported that brushite cements caused rapid decrease in pH in vivo after implantation [11, 48]. Therefore, the significant reduction of the ALP enzyme activity of dBMSCs on day 14 might occur because of cell death due to the rapid decrease in pH values during cell culture [50]. In addition, the ALP enzyme activity of 0% PLLA groups were significantly

lower than 5% PLLA group on day 14 ($p < 0.05$). This higher ALP enzyme activity of 5% PLLA group on day 14 was occurred because PLLA coating slowed down the release dissolution of DCPD resulting in the reduction of pH values of the medium. In addition, the ALP Enzyme will be further studied by normalizing with amount of protein release in the future.

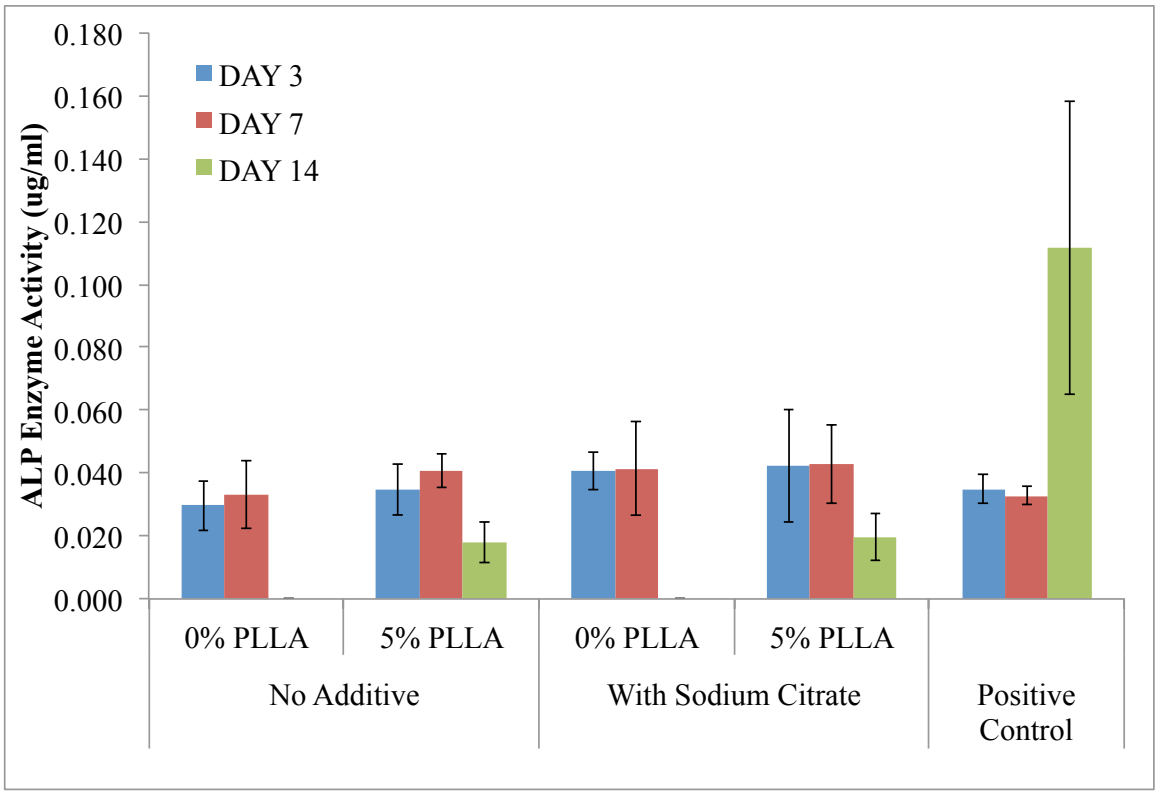

Figure 6.3 The quantitative measurement of alkaline phosphatase activity of dog bone marrow stromal stem cells cultured in the medium conditioned with DCPD or PLLA-coated DCPD samples. The standard DMEM medium was used as positive control.

7. CONCLUSION

From the results and discussions of this thesis on the dicalcium phosphate dihydrate (DCPD) and poly-L-lactide (PLLA)/DCPD composite, several important conclusions have been demonstrated as the following:

1. The effect of powder to liquid ratios (P/L), PLLA coating and sodium citrate on the mechanical properties of the DCPD cements.

As demonstrated in Fig. 3.6 and 3.7, the P/L ratios showed a significant effect on the diametral tensile strength because increasing P/L ratios resulting in the decrease of porosity. In addition, lower porosity leaded to the higher diametral tensile strength. Furthermore, decreasing porosity resulting in more compaction of the setting cements and higher mechanical strength.

As illustrated in Fig. 3.8, the PLLA coating was shown to have a significant effect on the fracture energy. The diametral compression test showed that DCPD samples failed and disintegrated due to their brittleness. However, the PLLA/DCPD composite samples retained an overall shape even though they failed mechanically. In addition, the 5% PLLA group was shown to achieve significant higher fracture energy than 0% PLLA group. Therefore, PLLA played an important role in improving the toughness of the samples by binding the samples into a whole piece.

As showed in Fig. 4.2, the sodium citrate played a crucial role in improving the diametral tensile strength of DCPD and PLLA/DCPD composite samples. Addition of sodium citrate as the setting regulator inhibits the growth of the DCPD crystals resulting in the increase of cements compaction by reducing the size of DCPD crystals.

Therefore, a combination of the increasing P/L ratios (1.00 to 1.50), the addition of 100 mM sodium citrate, and 5% PLLA coating resulted in the improvement of the diametral tensile strength of the DCPD samples from 0.50 ± 0.15 MPa to 2.70 ± 0.54 MPa. In addition, the fracture energy increased from 0.76 ± 0.18 N-mm to 12.67 ± 4.97 N-mm.

2. In vitro static degradation of DCPD and PLLA/DCPD composite samples (deionized water).

PLLA/DCPD samples did not show to be significantly different from DCPD samples during in vitro static degradation as mentioned in Chapter 5. The weight loss, pH changes, and fracture energy of the samples were found to be related to each other. The trends of the degradation behaviors for both DCPD and PLLA/DCPD composite samples were similar and occurred due to the three mechanisms: dissolution, disintegration, and conversion. The cements were first degraded due to dissolution and disintegration. Then, they stopped to degrade due to the saturated media. Finally, they started to degrade again due to HA conversion.

3. In vitro dynamic degradation of DCPD and PLLA/DCPD composite samples.

PLLA/DCPD samples did not show to be significantly different from DCPD samples during in vitro dynamic degradation as mentioned in Chapter 5. The DCPD and PLLA/DCPD samples (sodium citrate) were found to degrade faster than the samples (deionized water) as illustrated Fig. 5.7 during degradation because the sodium citrate inhibited the growth of the crystals resulting in smaller size of the crystals and more interface area between the crystals and media. As a result, the samples (sodium citrate) lost weight more than other groups (deionized Water) during degradation. The weight loss, pH changes, and fracture energy of the samples were found to be related to each other. As the immersion time increased, the overall weight loss curve tended to increase while the fracture energy tended to decrease.

4. In vitro cytoocompatibility of DCPD and PLLA/DCPD composite samples.

Fig. 6.1, 6.2 and 6.3 illustrated that the cells were able to proliferate and differentiate with the medium conditioned with both DCPD and PLLA-coated DCPD (deionized water and without sodium citrate). However, PLLA played an crucial role in the cell proliferation and differentiation study. The cells were found to proliferate and differentiate better in the well plate that contained medium conditioned with the PLLA/DCPD samples. The pH of the medium conditioned with DCPD samples rapidly decreased during the experiment resulted in cell death. Coating PLLA on the surface of DCPD samples slowed down the dissolution of DCPD cements caused by the pH reduction and more live cells. As a result, the cells were able to proliferate and differentiate better with the medium that conditioned with the PLLA/DCPD composite samples

LIST OF REFERENCES

LIST OF REFERENCES

[1] S. Bose and S. Tarafder, "Calcium phosphate ceramic systems in growth factor and drug delivery for bone tissue engineering: A review," *Acta Biomaterialia,* vol. 8, pp. 1401-1421, 2012.

[2] R. Langer and J. P. Vacanti, "Tissue engineering," *Science,* vol. 260, pp. 920-6, May 1993.

[3] K. J. L. Burg, S. Porter, and J. F. Kellam, "Biomaterial developments for bone tissue engineering," *Biomaterials* vol. 21, pp. 2347-2359, 2000.

[4] E. M. Younger and M. W. Chapman, Morbidity at bone graft donor sites," *JOURNAL OF ORTHOPAEDIC TRAUMA,* vol. 3, pp. 192-195, 1989.

[5] K. L. Low, S. H. Tan, S. H. Zein, J. A. Roether, V. Mourino, and A. R. Boccaccini, "Calcium phosphate-based composites as injectable bone substitute materials," *J Biomed Mater Res B Appl Biomater,* vol. 94, pp. 273-86, Jul 2010.

[6] W. E. Brown and L. C. Chow, "A new calcium phosphate setting cement," *J. Dent. Res.,* vol. 62, p. 672, 1983.

[7] R. Z. LeGeros, A. Chohayeb, and A. Shulman, "Apatitic calcium phosphates: possible dental restorative materials," *J. Dent. Res. ,* vol. 61, p. 343, 1982.

[8] F. Tamimi, Z. Sheikh, and J. Barralet, "Dicalcium phosphate cements: Brushite and monetite," *Acta Biomaterialia,* vol. 8, pp. 474-487, 2012.

[9] M. P. Ginebra, T. Traykova, and J. A. Planell, "Calcium phosphate cements as bone drug delivery systems: a review," *J Control Release,* vol. 113, pp. 102-10, Jun 2006.

[10] M. P. Ginebra, C. Canal, M. Espanol, D. Pastorino, and E. B. Montufar, "Calcium phosphate cements as drug delivery materials," *Adv Drug Deliv Rev,* vol. 64, pp. 1090-110, Sep 2012.

[11] E. M. Ooms, J. G. C. Wolke, M. T. van de Heuvel, B. Jeschke, and J. A. Jansen, "Histological evaluation of the bone response to calcium phosphate cement implanted in cortical bone," *Biomaterials,* vol. 24, pp. 989-1000, 2003.

[12] F. Theiss, D. Apelt, B. Brand, A. Kutter, K. Zlinszky, M. Bohner*, et al.*, "Biocompatibility and resorption of a brushite calcium phosphate cement," *Biomaterials,* vol. 26, pp. 4383-94, Jul 2005.

[13] U. Klammert, T. Reuther, C. Jahn, B. Kraski, A. C. Kubler, and U. Gbureck, "Cytocompatibility of brushite and monetite cell culture scaffolds made by three-dimensional powder printing," *Acta Biomater,* vol. 5, pp. 727-34, Feb 2009.

[14] M. Spangler, B. B. Phillips, and M. B. Ross, "Calcium Supplementation in Postmenopausal Women to Reduce the Risk of Osteoporotic Fractures," *American Journal of Health-System Pharmacy,* vol. 68, pp. 309-318, 2011.

[15] S. V. Dorozhkin, "Biocomposites and hybrid biomaterials based on calcium orthophosphates," *Biomatter,* vol. 1, pp. 3-56, Jul-Sep 2011.

[16] L. C. Chow, S. Hirayama, S. Takagi, and E. Parry, "Diametral tensile strength and compressive strength of a calcium phosphate cement: effect of applied pressure," *J Biomed Mater Res,* vol. 53, pp. 511-7, Sep 2000.

[17] M. P. Ginebra, M. Espanol, E. B. Montufar, R. A. Perez, and G. Mestres, "New processing approaches in calcium phosphate cements and their applications in regenerative medicine," *Acta Biomater,* vol. 6, pp. 2863-73, Aug 2010.

[18] D. L. Alge, G. Santa Cruz, W. S. Goebel, and T. M. Chu, "Characterization of dicalcium phosphate dihydrate cements prepared using a novel hydroxyapatite-based formulation," *Biomed Mater,* vol. 4, p. 025016, Apr 2009.

[19] M. G. Bohner, U., "Thermal Reactions of Brushite Cements," *J Biomed Mater Res B Appl Biomater,* vol. 84B, pp. 375-385, 2008.

[20] F. T. Mariño, J. Torres, M. Hamdan, C. R. Rodríguez, and E. L. Cabarcos, "Advantages of using glycolic acid as a retardant in a brushite forming cement," *Journal of Biomedical Materials Research Part B: Applied Biomaterials,* vol. 83B, pp. 571-579, 2007.

[21] A. P. Legrand, H. Sfihi, N. Lequeux, and J. Lemaître, "31P Solid-State NMR study of the chemical setting process of a dual-paste injectable brushite cements," *Journal of Biomedical Materials Research Part B: Applied Biomaterials,* vol. 91B, pp. 46-54, 2009.

[22] S. V. Dorozhkin, "Self-Setting Calcium Orthophosphate Formulations: Cements, Concretes, Pastes and Putties," *International Journal of Materials and Chemistry,* vol. 1, pp. 1-48, 2012.

[23] M. P. Hofmann, A. R. Mohammed, Y. Perrie, U. Gbureck, and J. E. Barralet, "High-strength resorbable brushite bone cement with controlled drug-releasing capabilities," *Acta Biomater,* vol. 5, pp. 43-9, Jan 2009.

[24] A. J. Ambard and L. Mueninghoff, "Calcium phosphate cement: review of mechanical and biological properties," *J Prosthodont,* vol. 15, pp. 321-8, Sep-Oct 2006.

[25] R. A. Sousa, J. F. Mano, R. L. Reis, A. M. Cunha, and M. J. Bevis, "Mechanical performance of starch based bioactive composite biomaterials molded with preferred orientation," *Polymer Engineering & Science,* vol. 42, pp. 1032-1045, 2002.

[26] N. J. S. Gorst, Y. Perrie, U. Gbureck, A. L. Hutton, M. P. Hofmann, L. M. Grover*, et al.*, "Effects of fibre reinforcement on the mechanical properties of brushite cement," *Acta Biomaterialia,* vol. 2, pp. 95-102, 2006.

[27] D. L. Alge and T. M. Chu, "Calcium phosphate cement reinforcement by polymer infiltration and in situ curing: a method for 3D scaffold reinforcement," *J Biomed Mater Res A,* vol. 94, pp. 547-55, Aug 2010.

[28] D. L. Alge, J. Bennett, T. Treasure, S. Voytik-Harbin, W. S. Goebel, and T. M. Chu, "Poly(propylene fumarate) reinforced dicalcium phosphate dihydrate cement composites for bone tissue engineering," *J Biomed Mater Res A,* vol. 100, pp. 1792-802, Jul 2012.

[29] X. Pang, X. Zhuang, Z. Tang, and X. Chen, "Polylactic acid (PLA): research, development and industrialization," *Biotechnol J,* vol. 5, pp. 1125-36, Nov 2010.

[30] R. K. Kullkarni, K. C. Pani, C. Neuman, and F. Leonard, "Polylactic acid for surgical implants," *Arch Surg* vol. 93, pp. 839-843, 1966.

[31] D. L. Alge, W. S. Goebel, and T. M. Chu, "Effects of DCPD cement chemistry on degradation properties and cytocompatibility: comparison of MCPM/beta-TCP and MCPM/HA formulations," *Biomed Mater,* vol. 8, p. 025010, Apr 2013.

[32] M. H. Alkhraisat, F. T. Marino, J. R. Retama, L. B. Jerez, and E. Lopez-Cabarcos, "Beta-tricalcium phosphate release from brushite cement surface," *J Biomed Mater Res A,* vol. 84, pp. 710-7, Mar 1 2008.

[33] L. Grover, "In vitro ageing of brushite calcium phosphate cement," *Biomaterials,* vol. 24, pp. 4133-4141, 2003.

[34] L. M. Grover, U. Gbureck, A. J. Wright, M. Tremayne, and J. E. Barralet, "Biologically mediated resorption of brushite cement in vitro," *Biomaterials,* vol. 27, pp. 2178-85, Apr 2006.

[35] M. Bohner, F. Theiss, D. Apelt, W. Hirsiger, R. Houriet, G. Rizzoli*, et al.*, "Compositional changes of a dicalcium phosphate dihydrate cement after implantation in sheep," *Biomaterials,* vol. 24, pp. 3463-3474, 2003.

[36] F. Carneiro and A. Barcellos, "Barcellos A. Re´sistance a` la traction des be´-tons," *Rilem Bull,* vol. 13, pp. 97-126, 1953.

[37] L. P. Van, C. Lowe, and C. Lemaitre, "Optimization of setting time and mechanical strength of β-TCP/MCPM cements," *Bioceramics,* vol. 10, pp. 477-480, 1997.

[38] Y. Kang, A. Scully, D. A. Young, S. Kim, H. Tsao, M. Sen*, et al.*, "Enhanced mechanical performance and biological evaluation of a PLGA coated beta-TCP composite scaffold for load-bearing applications," *Eur Polym J,* vol. 47, pp. 1569-1577, Aug 2011.

[39] M. Peroglio, L. Gremillard, J. Chevalier, L. Chazeau, C. Gauthier, and T. Hamaide, "Toughening of bio-ceramics scaffolds by polymer coating," *Journal of the European Ceramic Society,* vol. 27, pp. 2679-2685, 2007.

[40] Y. Kang, Y. Yao, G. Yin, Z. Huang, X. Liao, X. Xu*, et al.*, "A study on the in vitro degradation properties of poly(L-lactic acid)/beta-tricalcuim phosphate (PLLA/beta-TCP) scaffold under dynamic loading," *Med Eng Phys,* vol. 31, pp. 589-94, Jun 2009.

[41] A. A. Mirtchi and J. Lemaitre, "Calciumphosphate cementsaction of setting regulators on the properties of the p-tricalciumphosphate- monocalciumphosphate cements," *Biomaterials,* vol. 10, pp. 634-638, 1989.

[42] K. Ishikawa and K. Asaoka, "Estimation of ideal mechanical strength and critical porosity of calcium phosphate cement," *Journal of Biomedical Materials Research,* vol. 29, pp. 1537-1543, 1995.

[43] J. Zhao, X. Lu, K. Duan, L. Y. Guo, S. B. Zhou, and J. Weng, "Improving mechanical and biological properties of macroporous HA scaffolds through composite coatings," *Colloids and Surfaces B: Biointerfaces,* vol. 74, pp. 159-166, 2009.

[44] G. Pezzotti and S. M. F. Asmus, "Fracture behavior of hydroxyapatite/polymer interpenetrating network composites prepared by in situ polymerization process," *Materials Science and Engineering: A,* vol. 316, pp. 231-237, 2001.

[45] F. He and J. Ye, "In vitro degradation, biocompatibility, and in vivo osteogenesis of poly(lactic-co-glycolic acid)/calcium phosphate cement scaffold with unidirectional lamellar pore structure," *J Biomed Mater Res A,* vol. 100, pp. 3239-50, Dec 2012.

[46] M. Bohner, P. Van Landuyt, H. P. Merkle, and J. Lemaitre, "Composition effects on the pH of a hydraulic calcium phosphate cement," *J Mater Sci Mater Med,* vol. 8, pp. 675-81, Nov 1997.

[47] A. A. Mirtchi, J. Lemaitre, and N. Terao, "Calcium phosphate cements: study of the beta-tricalcium phosphate--monocalcium phosphate system," *Biomaterials,* vol. 10, pp. 475-80, Sep 1989.

[48] J. M. Curran, J. A. Gallagher, and J. A. Hunt, "The inflammatory potential of biphasic calcium phosphate granules in osteoblast/macrophage co-culture," *Biomaterials,* vol. 26, pp. 5313-20, Sep 2005.

[49] Z. Huan and J. Chang, "Novel bioactive composite bone cements based on the beta-tricalcium phosphate-monocalcium phosphate monohydrate composite cement system," *Acta Biomater,* vol. 5, pp. 1253-64, May 2009.

[50] S. Matsuyama and J. C. Reed, "Mitochondria-dependent apoptosis and cellular pH regulation," *Cell Death and Differentiation,* vol. 7, pp. 1155-1165, 2000.